

ACCESS-OM2: The Consortium of Ocean-Sea Ice Modelling in Australia's global ocean and sea ice model

Andrew Kiss, Andy Hogg, Kial Stewart, Adele Morrison, Aidan Heerdegen (ANU);
Nicholas Hannah (Double Precision); Paul Spence, Matthew England, Ryan Holmes (UNSW);
Russell Fiedler, Simon Marsland, Peter Oke, Siobhan O'Farrell, Christopher Chapman (CSIRO);
Maxim Nikurashin, Fabio Dias (UTas); Petra Heil (AAD & ACE CRC, UTas);
Gary Brassington, Helen Beggs, Justin Freeman (BoM); Fanghua Wu (Beijing Climate Center);
Stephen Griffies (GFDL); James Munroe (Memorial U. Newfoundland)

TODO: consolidate author list and add anyone who's missing (order is arbitrary at this stage)

The latest version of this document is available from

GitHub: <https://github.com/OceansAus/ACCESS-OM2-1-025-010deg-report>

This version: typeset 2018-06-20 14:10:42 +10:00

Set 'gitinfo' boolean to 'true' in preamble to show git version information (doesn't work in Overleaf; you may also need to run RUNME.sh).

CONTRIBUTORS PLEASE NOTE:

- please sign up with GitHub and click “watch” on <https://github.com/OceansAus/ACCESS-OM2-1-025-010deg-report> to be kept informed of discussions
- to discuss aspects of the paper, please post an issue at <https://github.com/OceansAus/ACCESS-OM2-1-025-010deg-report/issues> instead of using email. You can tag relevant parts of the .tex file with `\ISSUE{num}` (where “num” is the issue number) to link to the issue page (change tag to `\CISSUE{num}` if the issue is closed, so it is easily changed back if the issue is reopened).
- note contributors for sections in the .tex file with `\CONTRIBUTORS{...}`
- add “to do” items to the .tex file with `\TODO{...}`
- note errors and problems with `\FIXME{...}` in the .tex file
- to make git diffs easier, please try to write each sentence in the .tex file on a separate line
- use a bare number (no leading v) if you do git tags (for compatibility with the gitinfo2 package used here)
- see <https://github.com/OceansAus/ACCESS-OM2-1-025-010deg-report> for how to add or edit figures

Contents

1	Purpose of this document	4
2	Introduction	4
3	Model Configuration	4
3.1	Overview	4
3.2	MOM configuration	4
3.2.1	Vertical grid	4
3.2.2	Horizontal grid	5
3.2.3	Bathymetry	5
3.2.4	Other model physical parameters	6
3.3	CICE sea ice model configuration	6
3.3.1	Thickness redistribution	6
3.3.2	Dynamics	6
3.3.3	Thermodynamics	7
3.4	OASIS	7
3.5	Forcing	7
3.5.1	JRA55-do and repeat-year forcing	7
3.5.2	CORE-NYF	8
3.5.3	Restoring	8
3.5.4	Bulk formulas used	8
3.5.5	YATM / MATM	8
3.6	Initial conditions and spinup	9
3.6.1	Online runoff remapping via kdtree	9
3.7	Model computational details and performance	9
3.8	Comparison with similar models	9
3.8.1	GFDL CM2, CM2.5, CM2.6	9
3.8.2	ACCESS, ACCESS-CM2, ACCESS-ESM	9
3.8.3	OFAM3	10
3.8.4	MOM-SIS-01	10
3.8.5	UKMO GO6, GO7	10
3.8.6	RASM?	10
4	Model evaluation	10
4.1	Barotropic streamfunction	11
4.2	Surface current speed and variability	11
4.3	Transports through key straits and boundary currents	11
4.3.1	ITF	11
4.3.2	Drake Passage	11
4.3.3	Agulhas	11
4.4	Equatorial current velocity and temperature structure	11
4.5	Overturning	11
4.6	Meridional heat transport	11
4.7	Model bias assessments	12
4.8	Water mass properties and structure	12
4.8.1	T/S diagrams	12
4.8.2	Deep water formation / transformation rates, locations, properties	12
4.9	Heat conservation, bias and drift	12
4.9.1	SST bias	12
4.9.2	lat/depth T sections and bias	12
4.9.3	Drift: depth/time T hovmollers	12
4.9.4	zonally averaged surface heat flux terms	12

4.10	Salt conservation, bias and drift	12
4.10.1	SSS bias	13
4.10.2	lat/depth S sections and bias	13
4.10.3	Drift: depth/time S hovmollers	13
4.10.4	zonally averaged surface salt/freshwater flux terms	13
4.11	Variability	13
4.11.1	Western boundary current variability	13
4.11.2	EKE spatial distribution and wavenumber spectrum	13
4.12	Sea level	13
4.13	Sea ice	13
4.13.1	Seasonal cycle of extent, coverage and thickness distribution	14
4.13.2	Age	14
4.13.3	Formation rate	14
4.13.4	Drift	15
4.13.5	Ice deformation	15
4.13.6	Polynyas	15
4.14	Particularly important regions	15
4.14.1	ACC	15
4.14.2	East Australian Current	15
4.14.3	Leeuwin Current	15
4.14.4	North Atlantic	15
4.14.5	Arctic Ocean / Greenland-Iceland-Norway (GIN) Seas	15
4.14.6	Pacific	15
4.14.7	ITF	15
4.14.8	Agulhas	15
A	Auto-generated namelists	16
A.1	MOM namelist 'input.nml'	16
A.2	CICE namelists	26
A.2.1	cice_in.nml	26
A.2.2	input_ice.nml	33
A.2.3	input_ice.gfdl.nml	34
A.2.4	input_ice.monin.nml	35
A.3	MATM namelist 'input_atm.nml'	35
B	Auto-generated tables of namelist changes within runs	36
C	Auto-generated tables of namelist differences from ACCESS, ACCESS-CM2, ACCESS-ESM, OFAM	36
C.1	ACCESS-OM2-01 MOM compared to OFAM3	36
C.2	ACCESS-OM2-01 MOM compared to MOM-SIS-01 and GFDL	36
C.3	ACCESS-OM2-01 CICE compared to RASM and NCAR	36

List of Figures

1	Global overturning circulation on density surfaces (σ_2) for ACCESS-OM2 simulations at (a) 1° resolution; (b) 0.25° resolution and (c) 0.1° resolution.	12
2	Ice volume in each category at 0.1° resolution. The solid line shows the annual average.	14
3	Seasonal cycle of ice extent at 0.1° resolution.	14

Model	n	Δz_{\min} (m)	Δz_{\max} (m)	H_{\max} (m)
ACCESS-OM2	50	10.0	334.7	6000.0
ACCESS-OM2-025	50	10.1	209.9	5500.0
ACCESS-OM2-01	75	1.1	198.4	5808.7

Table 2: Vertical grid parameters: n levels, with spacing of Δz_{\min} and Δz_{\max} at the surface and maximum depth H_{\max} , respectively. **TODO:** these are discretised values from ocean_vgrid.nc - check that I'm correctly using the notation in Stewart et al. (2017)

1 Purpose of this document

This document serves two purposes:

1. This is a technical report to document the configuration and performance of the ACCESS-OM2 suite of models at 1, 0.25 and 0.1° horizontal resolution (<http://cosima.org.au/index.php/models/>), intended to be a resource for the user community (e.g. COSIMA) and readily updated. This approach was partly inspired by Griffies (2015).
2. This will form the basis of one or more journal papers to announce and assess the performance of these models, most likely to be submitted to GMD <https://www.geoscientific-model-development.net>

TODO: Auto-update figures by programatically running COSIMA notebooks, so you could have a jenkins job or somesuch checking the COSIMA tech paper notebooks are all up to date and working correctly <http://trittemio.github.io/smbits/2016/01/02/execute-notebooks/>

TODO: copy things from ARCCSS workshop poster, AMOS2018 talk, Bluelink talk, COSIMA workshop

2 Introduction

This technical report documents the ACCESS-OM2 ocean-sea ice model at nominal horizontal resolutions of 1°, 0.25° and 0.1°.

3 Model Configuration

CONTRIBUTORS: Andrew Kiss to coordinate

3.1 Overview

MOM, CICE, OASIS, JRA55

<http://www.mom-ocean.science> **TODO:** move to new web location

3.2 MOM configuration

The primary MOM 5 reference is Griffies (2012).

MOM parameters for the three model resolutions are tabulated in Appendix A.1. We discuss the choices of key parameters here.

Using conservative temperature for all but 1/10 which uses potential temp

TODO: cannibalise NCMAS application

3.2.1 Vertical grid

See table 2.

Discuss KDS vertical grid Stewart et al. (2017)

TODO: update? Kial is setting up KDS50 at 1°

discuss partial cells

ACCESS-OM2 uses GFDL50 **FIXME: wrong? doesn't match GFDL50 in table 1 of Stewart et al. (2017)** 50 levels, 10.0m spacing in top 200m then increasing smoothly to 334.7m by the bottom at 6000m.
 ACCESS-OM2-025 uses KDS50 **FIXME: wrong? doesn't match KDS50 in table 1 of Stewart et al. (2017)** 50 levels, 10.1m spacing at surface, increasing smoothly to 209.9m by the bottom at 5500m.
 ACCESS-OM2-01: KDS75 **TODO: check: maximum spacing and depth slightly different from KDS75** 75 levels, 1.1m spacing at surface, increasing smoothly to 198.4m by the bottom at 5808.7m.
TODO: figure showing grid spacing vs depth for ACCESS_OM2 models and others for comparison

3.2.2 Horizontal grid

The grid covers the global ocean, extending from the north pole to 81°S. The grid is Mercator between 65°N – 65°S, and tripolar (Murray, 1996) north of 65°N, with tripoles placed on land at 65°N and -100°E, 80°E. **TODO: describe spacing south of 65S**

TODO: explain grid refinement at equator – 1° only?

TODO: plots of x and y grid spacing in the three models

https://github.com/mom-ocean/MOM5/blob/master/doc/web/user_guide.md: “The grid_spec file [/short/v45/aek156/access-om2/control/01deg_jra55_ryf] contains the following horizontal grid information: geographic location of T, E, C and N-cell (Tracer, East, Corner, and North cells), half and full cell lengths (in meters), rotation information between logical (i.e., grid oriented) and geographic east of cell. The complete description of the horizontal grid and namelist option is available in hgrid”

3.2.3 Bathymetry

CONTRIBUTORS: Russ Fiedler

plot bathymetry for the 3 resolutions – incl difference from gebco and from 0.1deg as maps, scatter plots, histograms

There are no ice cavities as these are not supported in MOM5.1.

Mention the integrity checks and scripts used to generate the data (e.g. in /g/data3/hh5/tmp/cosima/bathymetry/tools/common/) — should these be made publicly available?

1° and 0.25°

0.1° based on Gebco2014 30sec gridded data **FIXME: which version?**

http://www.gebco.net/data_and_products/gridded_bathymetry_data/gebco_30_second_grid/ The topo data used in the runs is

/short/v45/aek156/access-om2/input/mom_01deg/topog.nc also

/g/data3/hh5/tmp/cosima/bathymetry/topog_latest.nc

Topography ends at a vertical wall at the ice shelf edge (the calving line, not the grounding line). A narrow strip along the southern boundary of the model is all land because the latitude range of the model was chosen for consistency with the previous MOM-SIS bathymetry which stopped at the grounding line.

TODO: plot or stats on how much model bathy differs from gebco

TODO: mention main places where bathy tweaks were made – see /g/data3/hh5/tmp/cosima/bathymetry/README

TODO: check if this relevant to the bathy file we use: “Enforced minimum of 7 levels (approx 10m). Excavated not filled in so land mask kept. Partial cells: Enforced thickness of max(10,0.2*dz). If partial cell were thinner than half this then the cell was removed.” (

/g/data3/hh5/tmp/cosima/bathymetry/README)

Minimum depth = 10m

Partial cells: `ncdump -h /short/v45/aek156/access-om2/input/mom_01deg/topog.nc` yields

depth:minimum_depth = 10.43281f ; depth:minimum_levels = 7 ; depth:min_thick = 10.f ;

depth:min_frac = 0.2f ;

3.2.4 Other model physical parameters

Parameterisations (or not) for SGS eddies (GM, Redi), surface boundary layer, bottom boundary layer, tidal mixing, internal gravity wave mixing, etc
horizontal and vertical friction

The lateral boundary condition for velocity is no-slip, as a consequence of using a B-grid (Griffies, 2012).

equation of state

3.3 CICE sea ice model configuration

CICE parameters for the three model resolutions are tabulated in Appendix A.2. We discuss the choices of key parameters here.

CICE parameter sensitivities: Urrego-Blanco et al. (2016)

cf. Andrew Roberts RASM cice namelist (Petra email 6 June) **TODO: get permission** which was used in Cassano et al. (2017); Hamman et al. (2017); Jin et al. (2018); Roberts et al. (in review 2018) see Appendix C.3

See Andrew Roberts' comments on Roberts et al. (2015) in email from Petra email 6 June — inertial coupling can be essential for stability

3.3.1 Thickness redistribution

4 ice layers + 1 snow

5 thickness categories. We use kcatbound=0, so lower bound of ice categories is 0, 0.64, 1.39, 2.47, 4.57m (Hunke et al., 2015, table 2). For ridging we use we use krdg_partic=1.

3.3.2 Dynamics

TODO: check I (AK) haven't misunderstood anything here – this is based on only a quick skim of most of these papers

We are currently using “classic EVP” (kdyn = 1, revised_evp = .false.) (Hunke and Dukowicz, 1997, 2002; Hunke, 2001). This represents the ice by a viscoplastic (VP) rheology, to which a fictitious elastic term is added to facilitate efficient numerical convergence to the viscoplastic solution via damped elastic waves which are supposed to decay to negligible amplitude during ndte sub-timesteps within each dynamic timestep (Hunke et al., 2015, sections 3.5.2 and 4.4). Another CICE option is the “revised EVP” method (Bouillon et al., 2013; Hunke et al., 2015, section 3.5.3) which corrects an error in the “classic EVP” stress formulation and may also improve the convergence rate of the elastic sub-timesteps and reduce the incidence of spurious grid-aligned linear kinematic features (“leads”). **TODO: try this out?** Bouillon et al. (2013) argue that this is superior to using “classic EVP”, but see warnings by Kimmritz et al. (2017, 2015) that numerical instability may dominate over convergence as the greatest source of error. **FIXME: wrong references? they don't say this as far as I can see.**

There is an ongoing debate regarding the suitability of viscoplastic ice rheology, particularly to represent on fine scales (Nye, 1973; Weiss et al., 2007; Lindsay et al., 2003; Kwok et al., 2008; Girard et al., 2009; Dansereau et al., 2016; Hutter et al., 2018). An alternative supported by CICE is the elastic-anisotropic-plastic (EAP) model (Weiss and Schulson, 2009; Wilchinsky and Feltham, 2006; Tsamados et al., 2013), but this seems relatively untested and uncalibrated at this stage.

If we accept the VP formulation, there is also the question of how well the EVP sub-timestepping converges to the VP solution with no residual elastic wave effects. Like many comparable models we use ndte=120 sub-timestep iterations, but Losch and Danilov (2012); Lemieux et al. (2012); Kimmritz et al. (2017, 2015) show that full convergence may take thousands of iterations even with the revised EVP method (particularly at high resolution), which would be prohibitively expensive. We must therefore expect our sea ice stress distribution to contain artefacts due to residual elastic waves. These artefacts may include spurious grid-scale noise and long linear features in the shear and divergence fields (Lemieux et al., 2012).

see Lemieux and Tremblay (2009)

discuss linear kinematic features (leads): [Hutchings et al. \(2005\)](#); [Wang et al. \(2016a\)](#); [Wang and Wang \(2009\)](#); [Losch et al. \(2014\)](#)
turning angle is set to zero — is this reasonable? see [Park and Stewart \(2016\)](#); [McPhee \(2008\)](#); [Leppäranta \(2011\)](#) — we are using 10m ageostrophic winds and can resolve the ocean Ekman layer.
Ice-ocean drag coefficient: we use $\text{dragio}=0.00536$, very close to the measured value of 0.0054 measured at 0.5 m below first-year landfast ice by [Shirasawa and Ingram \(1997\)](#). A wide range of values have been used in the literature ([Lu et al., 2011](#); [Martinson and Wamser, 1990](#); [Leppäranta, 2011](#), table 5.3), but the coefficient also depends on the water velocity and depth at which it is measured, the ice roughness, and the upper ocean stratification ([Leppäranta, 2011](#); [Waters and Bruno, 1995](#)).

3.3.3 Thermodynamics

mushy ice: [Turner et al. \(2013\)](#)

See Andrew Roberts' comments on mushy thermo in email from Petra email 6 June

melt ponds? See Andrew Roberts' comments on melt ponds in email from Petra email 6 June

3.4 OASIS

OASIS3-MCT or OASIS-MCT2?

Nic's work on ESMF regridding

Regridding method - <https://github.com/OceansAus/access-om2/wiki/Creating-Remapping-Weights>

Should we use high-frequency coupling? CICE flag `highfreq` implements the RASM coupling method of [Roberts et al. \(2015, 2011\)](#); also see http://www.oc.nps.edu/NAME/RASM_overview.pdf

3.5 Forcing

JRA55-do v1.3 atmospheric forcing (1984-5, 1990-1 or 2003-4 repeat-year, 0.5625° , 3-hourly) in addition to CORE NYF (2° , 6-hourly)

3.5.1 JRA55-do and repeat-year forcing

JRA55-do user manual: [Tsujino et al. \(2018b\)](#)

Data available from https://esgf-node.llnl.gov/search/input4mips/?institution_id=MRI and on NCI at `/g/data1/ua8/JRA55-do/RYP/v1-3/*.nc`

For the latest information on the dataset status and citation: <http://goo.gl/r8up31>.

see http://amaterasu.ees.hokudai.ac.jp/~tsujino/JRA55-do-v1.3/00README_v1.3.1st JRA-55: [Kobayashi et al. \(2015\)](#) JRA55-do: [Tsujino \(2015b,a, 2016\)](#); [Tsujino et al. \(2018a\)](#), [Tsujino et al. \(2016\)](#)

<http://www.clivar.org/omdp/japan2016>

JRA55-do version 1.3 provides 3-hourly liquid and solid precipitation, downwelling surface longwave and shortwave radiation, sea level pressure, 10m wind velocity, specific humidity and air temperature on a TL319 grid, 0.5625° ($9/16^\circ$) resolution, and daily river flux at 0.25° resolution.

TODO: check: what do we use for glacier runoff? groundwater? evaporation? upwelling longwave radiation?

"Runoff from Greenland and Antarctica are replaced by climatological runoff. Greenland runoff is based on [Bamber et al. \(2012\)](#) and Antarctica runoff is based on [Depoorter et al. \(2013\)](#)."

(http://amaterasu.ees.hokudai.ac.jp/~tsujino/JRA55-do-v1.3/00README_v1.3.1st)

we made a start on this: <https://github.com/OceansAus/matm/issues/5>

should we / do we use this for runoff? [Suzuki et al. \(2017\)](#)

currently fresh water is input at the ice shelf edges.

cf. runoff (iceberg discharge scheme) used in ACCESS-CM2 - see AMOS2018 notes on Dave Bi's talk and <https://accessdev.nci.org.au/trac/wiki/CMIP6workshop> — this is discharged only at the surface. See Siobhan's email 2018-06-04

Runoff - incl distributed iceberg melt? Ask Adele? basal melt needs to be at depth - notebook p561.

We have the data but waiting on it being published. Veronique has regridded this - see email

2017-11-16 [Merino et al. \(2016\)](#) and [Depoorter et al. \(2013\)](#) Paul: "The Antarctic ice berg data is

published and the data is publicly available here: <http://neichin.github.io/personalweb/publications/> However, the Antarctic basal melt fluxes are not published yet and the data has not been made public." Also see [Merino et al. \(2018\)](#); [Donat-Magnin et al. \(2017\)](#); [Mathiot et al. \(2017\)](#); [Hammond and Jones \(2016\)](#) Runoff - what range of depths is used? Top 4 levels??

discuss choice of year for RYF — will use 1984-5 for high-res runs – refer to Kial's paper
These 12-month periods were identified as particularly "neutral": 1 May 1984 - 30 April 1985, 1 May 1990 - 30 April 1991, 1 May 2003 - 29 April 2004 (we keep 29 Feb 2004 and ditch 30 April 2004 so as to keep 365 days per year). We have run ocean-sea ice spinups forced by all three JRA55-do v1.3 repeat years at 1° but we are concentrating on 1984-5 for the 1/10° spinup as it has less of the warming signal and also gives us more of the JRA55 dataset for subsequent interannual runs.
Kial's email 2018-03-05:

-1st of January is in the peak of the northern winter and southern summer, meaning the variability in forcing fields (ie. weather) is quite high. This is a problem for surface buoyancy fluxes in the north Atlantic and Labrador & Nordic Sea regions, where NADW formation is notoriously sensitive to changes in surface forcing. The day of the year with lowest variability (least weather) is going to be closer to the equinoxes, and in JRA55 DO it turns out to be 1 May.

-The three candidate years have been selected as the 12-month periods with climate indices closest to neutral. The climate indices of interest are the SOI, SAM and NAO. Removing the criteria that a 12-month period follows the calendar year allows us to find "years" that are closer to climatologically neutral.

-Having the jump at 1 May allows us to run the model harder. The model tends to fall over at 1 Jan if the jump is there, meaning we have to back off the timestep and nurse it through. Having the jump at 1 May does not require any such nursing. Currently we are running the ACCESS-OM2 1° with 5400 sec timesteps from initialization and getting through 90 years per day.

TODO: plots of anomalies from climatology for the time-mean (or seasonal-mean) RYF forcing fields

3.5.2 CORE-NYF

3.5.3 Restoring

sea surface salinity restoring: salt_sfc_restore.nc from World Ocean Atlas 2013 v2
<https://www.nodc.noaa.gov/OC5/woa13/>; timescale set by salt_restore.tscale (we use 10 days) but what really matters is piston velocity
15m/300day ie 0.05m/day is GFDL's standard piston velocity (Griffies, 12 April 2018)
with 1.1m top cell and 10 days, we have 0.11 m/day ie restoring twice as strongly as GFDL
see <https://github.com/OceansAus/access-om2/issues/52> and
http://www.earthsystemmodeling.org/esmf_releases/last_built/ESMF_refdoc/node3.html#SECTION03020000000000000000
2nd order conservative interpolation: [Kritsikis et al. \(2017\)](#)

3.5.4 Bulk formulas used

- relative or absolute wind? see [Wu et al. \(2017\)](#) and
https://arccss.slack.com/archives/C6PP0GU9Y/p1511825314000106?thread_ts=1511802000.000465&cid=C6PP0GU9Y and
<https://jra55-do.slack.com/archives/C7LEZT4KY/p1511963905000047> - we are using relative wind - but where is this set?

3.5.5 YATM / MATM

MATM parameters for the three model resolutions are tabulated in Appendix A.3.

Table 3: ACCESS-OM2 updates and extends ACCESS-OM and OFAM3

	ACCESS-OM	OFAM3	ACCESS-OM2
Ocean	MOM 4.1	MOM 4.1	MOM 5.1
Sea ice	CICE 4.1	—	CICE 5.1
Coupler	OASIS 3.25	—	OASIS 3-MCT
Grid	global tripolar, z^*	75°S–75°N only, z^*	global tripolar, z^*
Resolution	1°, 360×300×50	0.1°, 3600×1500×51, $\Delta z=5-1000\text{m}$	1°, 360×300× (50, 75 or 100 levels) or 0.25°, 1440×1080×50, $\Delta z = 10.1-210\text{m}$ or 0.1°, 3600×2700×75, $\Delta z=1.1-198\text{m}$

3.6 Initial conditions and spinup

Initial condition is from World Ocean Atlas 2013 v2 <https://www.nodc.noaa.gov/OC5/woa13/>.

What's the sea ice initial condition? 3m at pole, dropping off with latitude equatorward?? - Siobhan
- parameter ice.ic = 'default' 'default' = latitude and sst dependent

https://github.com/OceansAus/cice5/blob/5583ce54fd8822c1b8aef0549090167ca5f36d10/source/ice_init.F90#L23 sets up ice where SST is cold, max 3m thick...? https://github.com/OceansAus/cice5/blob/5583ce54fd8822c1b8aef0549090167ca5f36d10/source/ice_init.F90#L1538

3.6.1 Online runoff remapping via kdtree

3.7 Model computational details and performance

Craig et al. (2014)?

cf. MOM-SIS-01: 50–60kSU/day? - check with Andy

1/10°: 1200 PUs for CICE + 4358 PUs for MOM + 1 for MATM **TODO: update**

TODO: cf. Matt Chamberlain's 2016 talk: global MOM-SIS at 1/10° and 50 levels, 960 CPUs (50x23 layout, 200 masked), dt=720s, month ~100min: http://cosima.org.au/wp-content/uploads/2016/06/ofam_global_mac_.pdf – this is as fast as ACCESS-OM2-01 but about 6x cheaper!

see layout in ocean/input.nml: plot MOM tiling, showing dry tiles and bathymetry for each resolution

see BLCKX, BLXKY in cice5/bld/config.nci.auscom.3600x2700 etc - plot CICE tiling, showing idle tiles for each resolution

3.8 Comparison with similar models

Namelists of MOM-based models are compared in Appendix C.

3.8.1 GFDL CM2, CM2.5, CM2.6

cf. CM2-1deg CM2.5 CM2.6 (they were MOM v5) and discuss resolving eddies: Griffies et al. (2015) Delworth et al. (2012) Dunne et al. (2012) Griffies (2015)

cf. CORE (Griffies et al., 2009), CORE-II (Danabasoglu et al., 2014)

minimum depth = 40m ?

3.8.2 ACCESS, ACCESS-CM2, ACCESS-ESM

See <https://accessdev.nci.org.au/trac/wiki/CMIP6workshop> There's an ACCESS-CM2 report available - ask Arnold Sullivan. And data is available on NCI to members of p66 and NCI access groups

cf. ACCESS Bi et al. (2013a,b); Dix et al. (2013)

Bi et al. (2013b)

cf. ACCESS-CM2 Bi et al. (2016), <http://cosima.org.au/wp-content/uploads/2016/06/BI-COSIMA-Hobart-20160526.ppt.pdf> - Uses same MOM, CICE and OASIS versions as ACCESS-CM2

cf. ACCESS-ESM

https://www.google.com.au/url?sa=t&rct=j&q=&esrc=s&source=web&cd=2&ved=0ahUKEwjvjsmH0rjZAhWEnpQKHb7VC-EQFgg0MAE&url=https%3A%2F%2Faccessdev.nci.org.au%2Ftrac%2Fraw-attachment%2Fwiki%2FScienceDay%2Fziehn_access_esm1.pdf&usg=AOvVaw1bYwLzey6vpy7g6v7W0aFO

3.8.3 OFAM3

cf. OFAM3 namelists - see Matt Chamberlain's email 28 May 2018

cf. oceanMAPS3.0 http://cosima.org.au/wp-content/uploads/2016/06/Brassington.Ocean_modelling_and_forecasting_v3.pptx.pdf

The vertical resolution has also been improved relative to OFAM3 (Oke et al., 2013) at nearly all depths, particularly at the surface and in the deep ocean, with 75 levels ranging from 1.1m thick at the surface to 198m thick at 5808m (compared to 51 levels ranging from 5m to 1000m thick currently in OFAM3/Bluelink). Of particular relevance for coastal studies is the improved vertical resolution in the upper ocean, with 31 levels in the top 200m and a minimum water depth of 10m (rather than 24 levels and a minimum depth of 15m for OFAM3), providing better resolution of shelf processes and a closer match to coastlines.

3.8.4 MOM-SIS-01

cf. MOM-SIS-01 Spence et al. (2017) - forced by 2° CORE NYF - 75 levels; ACCESS-OM2-01 has newer bathy, CICE, JRA55-do, and probably different vertical grid

3.8.5 UKMO GO6, GO7

cf UKMO GO6, GO7 Storkey et al. (2018) - based on NEMO.

GO7 has cavities under the ice shelves, whereas GO6 is similar to ACCESS-OM2-x in having no cavities and fresh water input at the ice shelf edges.

3.8.6 RASM?

Cassano et al. (2017); Hamman et al. (2017); Jin et al. (2018); Roberts et al. (in review 2018), http://www.oc.nps.edu/NAME/RASM_overview.pdf

Key RASM differences from ACCESS-OM2-01:

- ndte=600 (cf 120)
- highfreq=true
- differing pond parameters hs0 and rfracmax
- lots of differences in shortwave_nml
- differing thermo parameters chio, dSdt_slow_mode

4 Model evaluation

CONTRIBUTORS: Andy Hogg to coordinate

use obs dataset and methods from CLIVAR Repository for Evaluating Ocean Simulations?

<http://www.clivar.org/clivar-panels/omdp/reos>

cf Ocean Modelling CORE-II Special Issue (Virtual) <http://www.sciencedirect.com/science/journal/14635003/vsi/10PSR6J3BV4>

OMIP - Griffies et al. (2016) - does BOM/CSIRO already have code to do this for CMIP6? ask Marsland

cf Oke et al. (2013)

cf http://www.cesm.ucar.edu/working_groups/Ocean/metrics.html?

cf esmvaltool <https://www.esmvaltool.org/>

See Fanghua's observation comparison notebooks (should be on github) and also her presentation from 2018-01-25 and <https://github.com/FanghuaWu/cosima-cookbook/tree/master/notebooks>
maps of Smagorinsky biharmonic lateral viscosity? what is the viscous WBC width this implies? - note that lateral visc is increased near western boundary, even in 0.1° model: This is set by ncar_boundary_scaling in 'MOM5/src/mom5/ocean_param/lateral/ocean_bihgen_friction.F90'
see HighResMIP ([Haarsma et al., 2016](#))

4.1 Barotropic streamfunction

late separation of Kuroshio - cf. [Colin de Verdière and Ollitrault \(2016\)](#) seems to be due to WSC anomaly in RYF8485 - see Kial's emails 16 May 2018 - see 10 year mean in Bluelink presentation Kiss-Bluelink-March-2018.pdf **TODO: see if problem also appears at lower resolution - see AK-AMOS-2018-figures**

4.2 Surface current speed and variability

[Laurindo et al. \(2017\)](#) [Archer et al. \(2017a,b, 2018\)](#) [Wijeratne et al. \(2018\)](#)

4.3 Transports through key straits and boundary currents

use zigzag method in tripolar region? - see appendix C4 in [Griffies et al. \(2016\)](#)

TODO: output vertical sections at high spatiotemporal resolution in diag_table

4.3.1 ITF

4.3.2 Drake Passage

CONTRIBUTORS: Andy Hogg

cf. [Donohue et al. \(2016\)](#)

4.3.3 Agulhas

4.4 Equatorial current velocity and temperature structure

CONTRIBUTORS: Ryan Holmes

cf. TOGA?

4.5 Overturning

The overturning circulation on density surfaces for all three resolutions is shown in Fig. 1. This figure ...

[Farneti et al. \(2015\)](#)

[Lumpkin and Speer \(2007\)](#)

[Talley \(2013\)](#)

4.6 Meridional heat transport

CONTRIBUTORS: Ryan Holmes

AMOC: do transect at 26.5N to cf RAPID array <http://www.rapid.ac.uk/rapidmoc/> [Smeed et al. \(2018\)](#)

cf. [Newsom et al. \(2016\)](#)

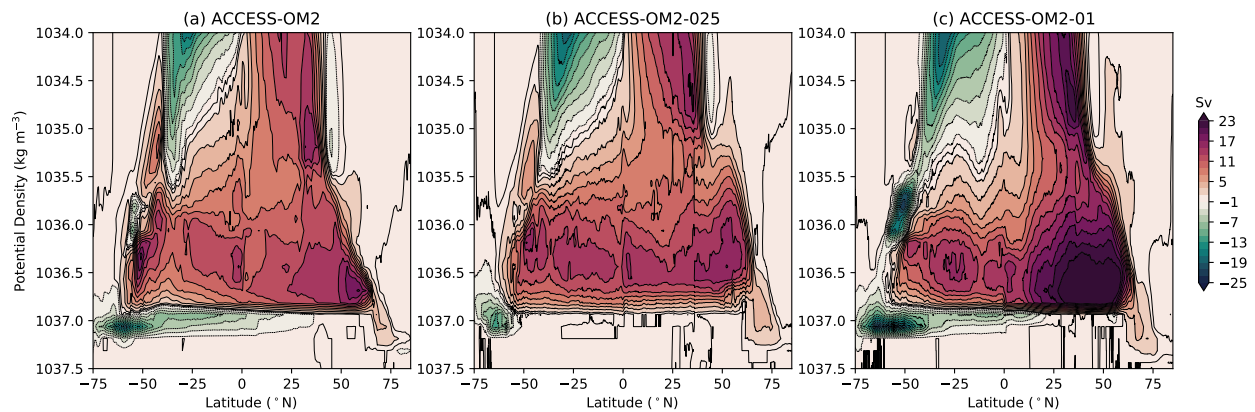


Figure 1: Global overturning circulation on density surfaces (σ_2) for ACCESS-OM2 simulations at (a) 1° resolution; (b) 0.25° resolution and (c) 0.1° resolution.

4.7 Model bias assessments

Minimal model bias important for BOM for data assimilation in oceanMAPS, but is difficult to assess with repeat-year forcing as the mean of RYF is not climatology, so after many repeats of RYF the slowly-adjusting ocean features will match neither climatology nor the state in the repeat year, even if the model itself is unbiased.

cf BRAN

cf [Kerry et al. \(2016\)](#)

4.8 Water mass properties and structure

mixed layer depth - Saltee et al JGR 2013 - climate models tend to underestimate winter mld

use Argo data

and MEOP southern ocean seal data <http://www.meop.net>

4.8.1 T/S diagrams

4.8.2 Deep water formation / transformation rates, locations, properties

[Farneti et al. \(2015\)](#) [Abernathy et al. \(2016\)](#) [Downes et al. \(2011\)](#)

4.9 Heat conservation, bias and drift

CONTRIBUTORS: Chris Chapman, Ryan Holmes

use XBT data from Chris Chapman?

cf FAFMIP? [Gregory et al. \(2016\)](#)

4.9.1 SST bias

4.9.2 lat/depth T sections and bias

4.9.3 Drift: depth/time T hovmollers

4.9.4 zonally averaged surface heat flux terms

4.10 Salt conservation, bias and drift

cf FAFMIP? [Gregory et al. \(2016\)](#)

4.10.1 SSS bias

4.10.2 lat/depth S sections and bias

4.10.3 Drift: depth/time S hovmollers

4.10.4 zonally averaged surface salt/freshwater flux terms

4.11 Variability

[Danabasoglu et al. \(2016\)](#)

4.11.1 Western boundary current variability

4.11.2 EKE spatial distribution and wavenumber spectrum

also check EKE spectrum to see if it follows the expected slope - eg [Capet et al. \(2008\)](#) cf. spectrum obs: [Xu and Fu \(2011\)](#)

4.12 Sea level

[Griffies et al. \(2014\)](#)

4.13 Sea ice

wavy ice features in 0.25deg — poor EVP convergence? <https://github.com/OceansAus/access-om2/issues/87>

Too much ice south of Svalbard in 0.10deg — **TODO: check Gulf Stream in 0.1deg – is it carrying heat far enough north?**

TODO: put probe points at narrowest point of northern Nares Str between Greenland and Ellesmere - compare ice export to Kwok et al. (2010)

Reanalyses for possible comparison with model (from Helen Beggs' email 21 Mar 2018):

- Reanalyses of sea ice observations: The OSI-SAF reanalysis is available in 10 km resolution from: <http://osisaf.met.no/p/ice/index.html#conc-reproc> It covers the period from 1978 to 2009 with consistent algorithm processing. PUM and validation reports are available at the website as well. OSI-SAF Daily sea ice concentration analyses are being ingested into the new Decadal OFAM Climate Model by Sakov and Sandery.
- <http://osisaf.met.no>: ice concentration, edge, drift and emissivity on both hemispheres, as well as climate consistent time series
- Bremen/Hamburg University and their AMSR2 based products
- NCEP (Bob Grumbine), <http://polar.ncep.noaa.gov/seaice/> - BoM uses NCEP 1/12° Daily Global Sea Ice Analyses as operational inputs into their SST analyses, used as the boundary condition to the NWP models

<http://psc.apl.uw.edu/research/projects/arctic-sea-ice-volume-anomaly/>

thickness: http://psc.apl.uw.edu/sea_ice_cdr/

see Ice_Validation_ACCESS-OM2-01.ipynb

https://github.com/aekiss/cosima-cookbook/blob/master/notebooks/Ice_Validation_ACCESS-OM2-01.ipynb uses data from <http://nsidc.org>

see SIMIP [Notz et al. \(2016\)](#)

see [Toyota and Kimura \(2018\)](#)

and check convergence [Bouillon et al. \(2013\)](#); [Kimmritz et al. \(2015\)](#); [Losch and Danilov \(2012\)](#);

[Lemieux and Tremblay \(2009\)](#)

[Wang et al. \(2016b\)](#)

[Downes et al. \(2015\)](#)

cf [Heil et al. \(2011\)](#) **ISSUE 3**

4.13.1 Seasonal cycle of extent, coverage and thickness distribution

ISSUE 1 ISSUE 2

NOAA/NSIDC Climate Data Record of Passive Microwave Sea Ice Concentration, Version 3

<http://nsidc.org/data/G02202>

Sea Ice Index, Version 3 <http://nsidc.org/data/g02135> See Figure 2: the growth of Arctic ice volume is due to increasing category 5, presumably due to ridging. We use kcatbound=0, so lower bound of ice categories is 0, 0.64, 1.39, 2.47, 4.57m (Hunke et al., 2015, table 2). So by year 9 most of the ice volume (not area) is more than 4.57m thick, including in the summer minimum.

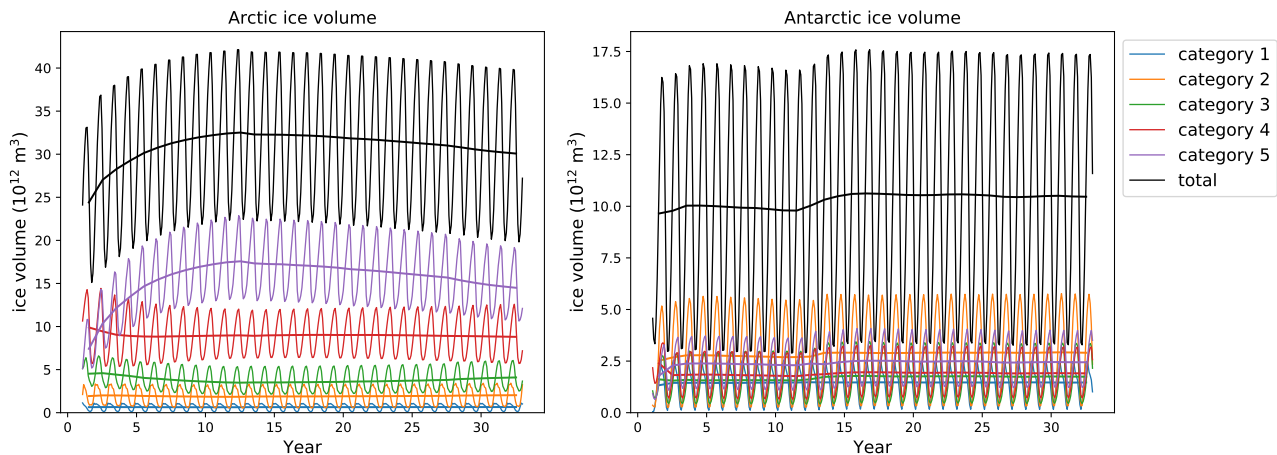


Figure 2: Ice volume in each category at 0.1° resolution. The solid line shows the annual average.

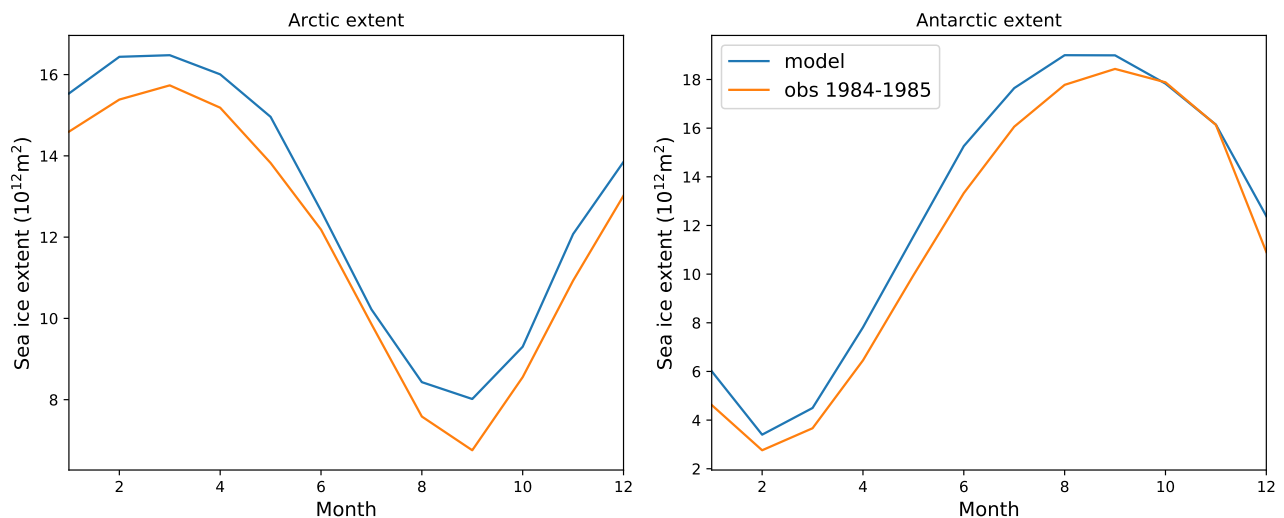


Figure 3: Seasonal cycle of ice extent at 0.1° resolution.

4.13.2 Age

4.13.3 Formation rate

ice production rate in coastal polynyas (Tamura et al., 2008; Tamura and Ohshima, 2011; Tamura et al., 2016; Nihashi and Ohshima, 2015; Ohshima et al., 2016) - see Adele's email 9 Mar 2018 - includes a script and netcdf version. Looks like you can download the data set here: <http://www.lowtem.hokudai.ac.jp/wwwod/polar-seaflux/> what diagnostics give us production in CICE? f.congel gives basal growth – not relevant? meltb, meltl, melts, meltt? frazil?

4.13.4 Drift

4.13.5 Ice deformation

cf. [Hutchings et al. \(2011\)](#)

4.13.6 Polynyas

[Uotila et al. \(2013\)](#) [Girard et al. \(2009\)](#) [Kwok et al. \(2008\)](#)

4.14 Particularly important regions

4.14.1 ACC

[Rintoul \(2018\)](#)

cf SOSE [Mazloff et al. \(2010\)](#)

transport

EKE [Farneti et al. \(2015\)](#)

4.14.2 East Australian Current

[Laurindo et al. \(2017\)](#) [Archer et al. \(2017a,b, 2018\)](#) [Wijeratne et al. \(2018\)](#)

4.14.3 Leeuwin Current

[Wijeratne et al. \(2018\)](#)

4.14.4 North Atlantic

North Atlantic mean state [Danabasoglu et al. \(2014\)](#) and variability [Danabasoglu et al. \(2016\)](#)

4.14.5 Arctic Ocean / Greenland-Iceland-Norway (GIN) Seas

mixed layer depth

water properties

bottom water formation

bottom water transport over sills

[Wang et al. \(2016c\)](#) [Ilicak et al. \(2016\)](#)

4.14.6 Pacific

[Tseng et al. \(2016\)](#)

4.14.7 ITF

transports through straits - cf INSTANT array obs and [Sprintall et al. \(2009\)](#); [Hautala et al. \(2001\)](#)

Marsland 12 Apr 2018: ACCESS (1°) used Rayleigh drag to shift transport from westernmost to easternmost strait to match obs. Also cf. Perth-Jakarta line (XBT?)

4.14.8 Agulhas

transport, structure, variability

A Auto-generated namelists

These are auto-generated by `make_nml_tables.py` which uses `nmltab` (<https://github.com/aekiss/nmltab>). Variables are weblinks to source code searches. Variables that differ between the models are highlighted. Greyed values are ignored.

FIXME: these namelists are out of date

TODO: generate complete tables that include the default values of parameters not specified in namelists

A.1 MOM namelist 'input.nml'

Group	Variable	/short/ v45/ amh157/ access- om2/ control/ 1deg_- jra55_ryf/ ocean/ input.nml	/short/ v45/ aek156/ access- om2/ control/ 025deg_- jra55_ryf/ ocean/ input.nml	/short/ v45/ amh157/ access- om2/ control/ 01deg_- jra55_ryf/ ocean/ input.nml
auscom_ice_nml	<code>alice_cutoff</code>	0.15	0.15	0.15
	<code>chk_i2o_fields</code>	False	False	False
	<code>chk_o2i_fields</code>	False	False	False
	<code>do_ice_once</code>	False	False	False
	<code>dt_cpl</code>	3600	1200	150
	<code>fixmeltt</code>	False	False	False
	<code>frazil_factor</code>	1.0	1.0	1.0
	<code>iceform_adj_salt</code>	False	False	False
	<code>icemlt_factor</code>	1.0	1.0	1.0
	<code>kmxice</code>	5	5	5
	<code>pop_icediag</code>	True	True	True
	<code>redsea_gulfbay_sfix</code>	True		
	<code>sign_stflx</code>	1.0	1.0	1.0
	<code>tmelt</code>	-0.216	-0.216	-0.216
	<code>use_ioaice</code>	True	True	True
bg_diff_lat_dependence_nml	<code>bg_diff_eq</code>	1×10^{-6}		
	<code>lat_low_bgdiff</code>	20.0		
diag_manager_nml	<code>debug_diag_manager</code>		True	
	<code>issue_oor_warnings</code>	False	True	False
	<code>max_axes</code>			300
	<code>max_files</code>			1000
	<code>max_input_fields</code>			700
	<code>max_num_axis_sets</code>			40
	<code>max_output_fields</code>			700
fms_io_nml	<code>checksum_required</code>			False
	<code>fileset_write</code>	'single'	'single'	'multi'
	<code>max_files_r</code>			700
	<code>max_files_w</code>			700
	<code>threading_read</code>	'multi'	'multi'	'multi'
fms_nml	<code>threading_write</code>	'single'	'single'	'multi'
	<code>clock_grain</code>	'LOOP'	'LOOP'	'LOOP'
	<code>domains_stack_size</code>			115200
generic_tracer_nml	<code>print_memory_usage</code>			False
	<code>do_generic_cfc</code>			False
	<code>do_generic_topaz</code>			False
	<code>do_generic_tracer</code>			False

Group (continued)	Variable	/short/ v45/ amh157/ access- om2/ control/ 1deg- jra55_ryf/ ocean/ input.nml	/short/ v45/ aek156/ access- om2/ control/ 025deg- jra55_ryf/ ocean/ input.nml	/short/ v45/ amh157/ access- om2/ control/ 01deg- jra55_ryf/ ocean/ input.nml
mom_oasis3_interface.nml	fields_in	'u_flux', 'v_flux', 'lprec', 'fprec', 'salt_flux', 'mh_flux', 'sw_flux', 'q_flux', 't_flux', 'lw_flux', 'runof', 'p', 'aice', 'wfimelt', 'wiform'	'u_flux', 'v_flux', 'lprec', 'fprec', 'salt_flux', 'mh_flux', 'sw_flux', 'q_flux', 't_flux', 'lw_flux', 'runof', 'p', 'aice', 'wfimelt', 'wiform'	'u_flux', 'v_flux', 'lprec', 'fprec', 'salt_flux', 'mh_flux', 'sw_flux', 'q_flux', 't_flux', 'lw_flux', 'runof', 'p', 'aice', 'wfimelt', 'wiform'
	fields_out	't_surf', 's_surf', 'u_surf', 'v_surf', 'dssldx', 'dssldy', 'frazil'	't_surf', 's_surf', 'u_surf', 'v_surf', 'dssldx', 'dssldy', 'frazil'	't_surf', 's_surf', 'u_surf', 'v_surf', 'dssldx', 'dssldy', 'frazil'
	num_fields_in	15	15	15
	num_fields_out	7	7	7
	send_after_ocean_update	True	True	True
	send_before_ocean_update	False	False	False
monin_obukhov.nml	neutral		True	True
mpp_io.nml	deflate_level			5
	shuffle			1
ocean_adv_vel_diag.nml	diag_step	4320	4320	576
	large_cfl_value	10.0	10.0	10.0
	max_cfl_value	100.0	100.0	100.0
	verbose_cfl	True	True	True
ocean_advection_velocity.nml	max_advection_velocity	0.5	0.5	0.2
ocean_albedo.nml	ocean_albedo_option		2	2
ocean_barotropic.nml	barotropic_halo	10	10	10
	barotropic_time_stepping_a	True	True	True
	barotropic_time_stepping_b	False	False	False
	debug_this_module	False	False	False
	diag_step	4320	4320	576
	eta_max	8.0	8.0	8.0
	frac_crit_cell_height	0.2	0.2	0.2
	pred_corr_gamma	0.2	0.2	0.2
	smooth_eta_diag_laplacian	True	True	True
	smooth_eta_t_biharmonic	False	False	False
	smooth_eta_t_laplacian	True	True	True
	smooth_pbot_t_biharmonic	False	False	False
	smooth_pbot_t_laplacian	True	True	True
	truncate_eta	False	False	False
	use_legacy_barotropic_halos	False	False	False
	vel_micom_bih	0.01	0.01	0.01

Group (continued)	Variable	/short/ v45/ amh157/ access- om2/ control/ 1deg- jra55_ryf/ ocean/ input.nml	/short/ v45/ aek156/ access- om2/ control/ 025deg- jra55_ryf/ ocean/ input.nml	/short/ v45/ amh157/ access- om2/ control/ 01deg- jra55_ryf/ ocean/ input.nml
	vel_micom_lap	0.05	0.05	0.05
	vel_micom_lap_diag	0.2	0.2	0.5
	verbose_truncate	True	True	True
	zero_tendency		False	False
ocean_bbc_nml	bmf_implicit		True	True
	cdbot	0.001	0.001	0.001
	cdbot_hi		0.007	0.007
	cdbot_low_of_wall	False		
	cdbot_roughness_length		False	False
	cdbot_roughness_uamp		True	True
	uresidual		0.05	0.05
	use_geothermal_heating	False	False	False
ocean_bbc_ofam_nml	read_tide_speed	False		
	uresidual2_max	1.0		
ocean_bih_friction_nml	bih_friction_scheme	'general'	'general'	'general'
ocean_bih_tracer_nml	tracer_mix_micom		True	True
	use_this_module	False	False	False
	vel_micom		0.001	0.001
ocean_bihcst_friction_nml	use_this_module	False	False	False
ocean_bihgen_friction_nml	bottom_5point	True	False	False
	eq_lat_micom	0.0	0.0	0.0
	eq_vel_micom_aniso	0.0	0.0	0.0
	eq_vel_micom_iso	0.0	0.0	0.0
	equatorial_zonal	False	False	False
	k_smag_aniso	0.0	0.0	0.0
	k_smag_iso	2.0	2.0	2.0
	ncar_boundary_scaling	True	True	True
	ncar_boundary_scaling_read		True	True
	ncar_rescale_power	2	2	2
	ncar_vconst_4	2×10^{-8}	2×10^{-8}	2×10^{-8}
	ncar_vconst_5	5	5	5
	use_this_module	True	True	True
	vel_micom_aniso	0.0	0.0	0.0
	vel_micom_bottom	0.01	0.0	0.0
	vel_micom_iso	0.04	0.0	0.0
	visc_crit_scale	0.25	1.0	1.0
ocean_convect_nml	convect_full_scalar	False	True	True
	convect_full_vector	True	False	False
	use_this_module	False	False	False
ocean_coriolis_nml	acor	0.5	0.5	0.5
	use_this_module	True	True	True
ocean_density_nml	eos_linear	False	False	False
	eos_preteos10	True	True	True
	layer_nk	80	80	80
	neutralrho_max	1030.0	1038.0	1038.0
	neutralrho_min	1020.0	1028.0	1028.0
	potrho_max	1038.0	1038.0	1038.0
	potrho_min	1028.0	1028.0	1028.0
ocean_domains_nml	max_tracers	10	5	5
ocean_form_drag_nml	cprime_aiki	0.6		

Group (continued)	Variable	/short/ v45/ amh157/ access- om2/ control/ 1deg_- jra55_ryf/ ocean/ input.nml	/short/ v45/ aek156/ access- om2/ control/ 025deg_- jra55_ryf/ ocean/ input.nml	/short/ v45/ amh157/ access- om2/ control/ 01deg_- jra55_ryf/ ocean/ input.nml
	use_this_module	False	False	False
ocean_frazil_nml	debug_this_module		False	False
	frazil_only_in_surface		False	False
	freezing_temp_preteos10		True	True
	freezing_temp_simple	True	False	False
	use_this_module	True	True	True
ocean_grids_nml	debug_this_module	True	False	False
	read_rho0_profile	False		
ocean_increment_eta_nml	days_to_increment	0		
	fraction_increment	1.0		
	secs_to_increment	1800		
	use_this_module	False	False	False
ocean_increment_tracer_nml	days_to_increment	0		
	fraction_increment	1.0		
	secs_to_increment	1800		
	use_this_module	False	False	False
ocean_increment_velocity_nml	days_to_increment	0		
	fraction_increment	1.0		
	secs_to_increment	1800		
	use_this_module	False	False	False
ocean_lap_friction_nml	lap_friction_scheme	'general'	'general'	'general'
ocean_lap_tracer_nml	use_this_module	False	False	False
ocean_lapcst_friction_nml	use_this_module	False	False	False
ocean_lapgen_friction_nml	bottom_5point	True		
	k_smag_aniso	0.0		
	k_smag_iso	0.0	2.0	2.0
	ncar_only_equatorial	True		
	restrict_polar_visc	True		
	restrict_polar_visc_lat	60.0		
	restrict_polar_visc_ratio	0.35		
	use_this_module	True	False	False
	vconst_1	8 000 000.0		
	vconst_2	0.0		
	vconst_3	0.8		
	vconst_4	5×10^{-9}		
	vconst_5	3		
	vconst_6	300 000 000		
	vconst_7	100.0		
	vel_micom_iso	0.1		
	viscosity_ncar	True		
	viscosity_ncar_2000	False		
	viscosity_ncar_2007	True		
	viscosity_scale_by_rossby	True		
	viscosity_scale_by_rossby_power	4.0		
ocean_mixdownslope_nml	debug_this_module	False	False	False
	mixdownslope_mask_gfdl	False		
	mixdownslope_npts	4		
	read_mixdownslope_mask	False		
	use_this_module	True	False	False
ocean_model_nml	baroclinic_split	1	1	1

Group (continued)	Variable	/short/ v45/ amh157/ access- om2/ control/ 1deg- jra55_ryf/ ocean/ input.nml	/short/ v45/ aek156/ access- om2/ control/ 025deg- jra55_ryf/ ocean/ input.nml	/short/ v45/ amh157/ access- om2/ control/ 01deg- jra55_ryf/ ocean/ input.nml
	barotropic_split	80	80	80
	cmip_units	True	True	
	debug	False	False	False
	dt_ocean	3600	1200	150
	io_layout	4, 3	6, 5	10, 15
	layout	16, 15	48, 40	80, 75
	surface_height_split	1	1	1
	time_tendency	'twolevel'	'twolevel'	'twolevel'
	vertical_coordinate	'zstar'	'zstar'	'zstar'
ocean_momentum_source.nml	rayleigh_damp_exp_from_bottom		False	False
	use_rayleigh_damp_table	True	True	True
	use_this_module	True	True	True
ocean_nphysics.nml	debug_this_module	False	False	False
	use_nphysicsa	False	False	False
	use_nphysicsb	False	False	False
	use_nphysicsc	True	False	False
	use_this_module	True	False	False
ocean_nphysics_util.nml	agm	600.0	100.0	100.0
	agm_closure	True	True	True
	agm_closure_baroclinic	True	True	True
	agm_closure_buoy_freq	0.004	0.004	0.004
	agm_closure_eady_ave_mixed	True		
	agm_closure_eady_cap	True		
	agm_closure_eady_smooth_horz	True		
	agm_closure_eady_smooth_vert	True		
	agm_closure_eddy_gamma	0.0		
	agm_closure_eddy_greatbatch	False		
	agm_closure_grid_scaling	True		
	agm_closure_length	50 000.0	50 000.0	50 000.0
	agm_closure_length_bczone	False	False	False
	agm_closure_length_fixed	False	False	False
	agm_closure_length_rossby	False	False	False
	agm_closure_lower_depth	2000.0	2000.0	2000.0
	agm_closure_max	600.0	600.0	600.0
	agm_closure_min	50.0	100.0	100.0
	agm_closure_scaling	0.07	0.07	0.07
	agm_closure_upper_depth	100.0	100.0	100.0
	agm_damping_time	45.0		
	agm_smooth_space	False		
	agm_smooth_time	False		
	aredi	600.0	600.0	600.0
	aredi_equal_agm	False	False	False
	drhodz_mom4p1	True	False	False
	drhodz_smooth_horz	False	False	False
	drhodz_smooth_vert	False	False	False
	nphysics_util_zero_init	True		
	rossby_radius_max	100 000.0	100 000.0	100 000.0
	rossby_radius_min	15 000.0	15 000.0	15 000.0
	smax		0.002	0.002
	swidth		0.002	0.002
	tracer_mix_micom	False	False	False

Group (continued)	Variable	/short/ v45/ amh157/ access- om2/ control/ 1deg- jra55_ryf/ ocean/ input.nml	/short/ v45/ aek156/ access- om2/ control/ 025deg- jra55_ryf/ ocean/ input.nml	/short/ v45/ amh157/ access- om2/ control/ 01deg- jra55_ryf/ ocean/ input.nml
	vel_micom	0.0	0.0	0.0
ocean_nphysicsa_nml	use_this_module	False	False	False
ocean_nphysicsb_nml	use_this_module	False	False	False
ocean_nphysicsc_nml	bv_freq_smooth_vert	True		
	bvp_bc_mode	2		
	bvp_min_speed	0.1		
	bvp_speed	0.0		
	debug_this_module	False		
	do_gm_skewsion	True		
	do_neutral_diffusion	True		
	epsln_bv_freq	1 × 10 ⁻¹²		
	gm_skewsion_bvproblem	True		
	gm_skewsion_modes	False		
	neutral_eddy_depth	True		
	neutral_physics_limit	True		
	number_bc_modes	2		
	regularize_psi	False		
	smax_psi	0.01		
	smooth_psi	True		
	tmask_neutral_on	True		
	turb_blayer_min	50.0		
	use_this_module	True	False	False
ocean_operators_nml	use_legacy_div_ud		False	False
ocean_overexchange_nml	debug_this_module	False	False	False
	overexch_check_extrema	False		
	overexch_npts	4	4	4
	overexch_weight_far	False	False	False
	overflow_umax	5.0	5.0	5.0
	use_this_module	False	False	False
ocean_overflow_nml	debug_this_module	False	False	False
	use_this_module	False	False	False
ocean_overflow_ofp_nml	debug_this_module		False	False
	diag_step		4320	5760
	do_entrainment_para_ofp		False	False
	do_mass_ofp		True	True
	frac_exchange_src		1.0	1.0
	max_vol_trans_ofp		10 000 000.0	10 000 000.0
	use_this_module		False	False
ocean_polar_filter_nml	use_this_module	False	False	False
ocean_pressure_nml	zero_pressure_force		False	False
ocean_rivermix_nml	debug_this_module	False	False	False
	river_diffuse_salt	False	False	True
	river_diffuse_temp	False	False	True
	river_diffusion_thickness	0.0	0.0	0.0
	river_diffusivity	0.0	0.0	0.0
	river_insertion_thickness	40.0	40.0	40.0
	use_this_module	True	True	True
ocean_riverspread_nml	debug_this_module			False
	use_this_module	True	False	True

Group (continued)	Variable	/short/ v45/ amh157/ access- om2/ control/ 1deg_- jra55_ryf/ ocean/ input.nml	/short/ v45/ aek156/ access- om2/ control/ 025deg_- jra55_ryf/ ocean/ input.nml	/short/ v45/ amh157/ access- om2/ control/ 01deg_- jra55_ryf/ ocean/ input.nml
ocean_rough_nml	rough_scheme		'beljaars'	'beljaars'
ocean_sbc_nml	avg_sfc_temp_salt_eta	True	True	True
	avg_sfc_velocity	True	True	True
	calvingspread		False	False
	do_bitwise_exact_sum		False	False
	do_flux_correction		False	False
	land_model_heat_fluxes		False	False
	max_delta_salinity_restore	0.5	0.5	0.5
	max_ice_thickness	8.0	0.0	0.0
	read_restore_mask	False	False	False
	restore_mask_gfdl	False	False	False
	runoff_salinity	0.0	0.0	0.0
	salt_correction_scale		0.0	0.0
	salt_restore_as_salt_flux	True	True	True
	salt_restore_tscale	15.0	60.0	60.0
	salt_restore_under_ice	True	True	True
	temp_restore_tscale	-1.0	-10.0	-10.0
	use_full_patm_for_sea_level		False	False
	use_waterflux	True	True	True
	waterflux_tavg	False		
	zero_heat_fluxes	False	False	False
	zero_net_salt_correction		False	False
	zero_net_salt_restore	True	True	True
	zero_net_water_correction		False	False
	zero_net_water_couple_restore	True	True	True
	zero_net_water_coupler	True	True	True
	zero_net_water_restore	True	True	True
	zero_surface_stress	False	False	False
	zero_water_fluxes	False	False	False
ocean_sbc_ofam_nml	restore_mask_ofam	False		
	river_temp_ofam	False		
ocean_shortwave_csiro_nml	debug_this_module		False	
	read_depth	True	True	
	use_this_module	True	False	False
	zmax_pen	7000	7000	
ocean_shortwave_gfdl_nml	debug_this_module	False	False	False
	enforce_sw_frac	True	True	True
	optics_manizza	True	True	True
	optics_morel_antoine		False	False
	read_chl	False	True	True
	sw_pen_fixed_depths	False		
	use_this_module	False	True	True
	zmax_pen	200.0	300.0	300.0
ocean_shortwave_jerlov_nml	use_this_module	False	False	False
ocean_shortwave_nml	use_shortwave_csiro	True	False	False
	use_shortwave_gfdl	False	True	True
	use_shortwave_jerlov	False	False	False
	use_this_module	True	True	True
ocean_sigma_transport_nml	sigma_advection_on	False	False	False
	sigma_advection_sgs_only	False	False	False

Group (continued)	Variable	/short/ v45/ amh157/ access- om2/ control/ 1deg- jra55_ryf/ ocean/ input.nml	/short/ v45/ aek156/ access- om2/ control/ 025deg- jra55_ryf/ ocean/ input.nml	/short/ v45/ amh157/ access- om2/ control/ 01deg- jra55_ryf/ ocean/ input.nml
	sigma_diffusion_on	True	True	True
	sigma_diffusivity_ratio	1×10^{-6}	1×10^{-6}	1×10^{-6}
	sigma_just_in_bottom_cell	True	True	True
	sigma_umax	0.01	0.01	0.01
	smooth_sigma_thickness	True	True	True
	smooth_sigma_velocity	True	True	True
	smooth_velmicom	0.2	0.2	0.2
	thickness_sigma_layer	100.0	100.0	100.0
	thickness_sigma_max	100.0	100.0	100.0
	thickness_sigma_min	100.0	100.0	100.0
	tmask_sigma_on	False	False	False
	tracer_mix_micom	True	True	True
	use_this_module	True	False	False
	vel_micom	0.05	0.05	0.05
ocean_solo_nml	calendar	'NOLEAP'	'NOLEAP'	'NOLEAP'
	date_init	1, 1, 1, 0, 0, 0	1, 1, 1, 0, 0, 0	1, 1, 1, 0, 0, 0
	days	1460	31	30
	debug_this_module	False		
	dt_cpld	3600	1200	150
	hours	0	0	0
	minutes	0	0	0
	months	0	0	0
	seconds	0	0	0
	years	0	0	0
ocean_sponges_eta_nml	use_this_module	False	False	False
ocean_sponges_tracer_nml	damp_coeff_3d	False	False	False
	use_this_module	False	False	False
ocean_sponges_velocity_nml	use_this_module	False	False	False
ocean_submesoscale_nml	coefficient_ce		0.05	0.05
	debug_this_module	False	False	False
	front_length_const	5000.0	5000.0	5000.0
	front_length_deform_radius	True	True	True
	limit_psi	True	True	True
	limit_psi_velocity_scale	0.5	0.5	0.5
	min_kblt	4	4	4
	smooth_advect_transport		True	True
	smooth_advect_transport_num		4	4
	smooth_hblt	False	False	False
	smooth_psi		True	True
	smooth_psi_num		3	3
	submeso_advect_flux		False	False
	submeso_advect_limit		True	True
	submeso_advect_upwind		True	True
	submeso_advect_zero_bdy		True	True
	submeso_diffusion		False	False
	submeso_diffusion_biharmonic		True	True
	submeso_diffusion_scale		10.0	10.0
	submeso_limit_flux	True		
	submeso_skew_flux		True	True

Group (continued)	Variable	/short/ v45/ amh157/ access- om2/ control/ 1deg- jra55_ryf/ ocean/ input.nml	/short/ v45/ aek156/ access- om2/ control/ 025deg- jra55_ryf/ ocean/ input.nml	/short/ v45/ amh157/ access- om2/ control/ 01deg- jra55_ryf/ ocean/ input.nml
	use_hblt_equal_mld	True	True	True
	use_psi_legacy		False	False
	use_this_module	True	True	True
ocean_tempsalt_nml	debug_this_module	False	False	True
	pottemp_2nd_iteration	True	True	True
	pottemp_equal_contemp		True	True
	s_max	55.0	70.0	70.0
	s_max_limit	42.0	42.0	42.0
	s_min	-1.0	0.0	0.0
	s_min_limit	0.0	2.0	2.0
	t_max	55.0	55.0	55.0
	t_max_limit	32.0	32.0	32.0
	t_min	-5.0	-20.0	-20.0
	t_min_limit	-2.0	-5.0	-5.0
	temperature_variable	'conservative temp'	'potential_ temp'	'potential_ temp'
ocean_thickness_nml	debug_this_module	False	False	False
	debug_this_module_detail	False	False	False
	initialize_zero_eta	False		
	read_rescale_rho0_mask	False		
	rescale_mass_to_get_ht_mod		False	False
	rescale_rho0_basin_label	7.0		
	rescale_rho0_mask_gfdl	False		
	rescale_rho0_value	0.75		
	thickness_dzt_min	1.0	2.0	2.0
	thickness_dzt_min_init	2.0	10.0	10.0
	thickness_method	'energetic'	'energetic'	'energetic'
ocean_topog_nml	min_thickness	25.0		
ocean_tracer_advect_nml	advect_sweby_all	True		
	async_domain_update	True		
	debug_this_module	False	False	False
	read_basin_mask		False	False
ocean_tracer_diag_nml	diag_step	4320	4320	576
	do_bitwise_exact_sum	False	False	False
	tracer_conserve_days	1.0	30.0	30.0
ocean_tracer_nml	age_tracer_max_init	0.0	0.0	0.0
	debug_this_module	False	False	False
	frazil_heating_after_vphysics	True	True	True
	frazil_heating_before_vphysics	False	False	False
	limit_age_tracer	True	True	True
	remap_depth_to_s_init	False	False	False
	use_tempsalt_check_range	True	True	True
	zero_tendency	False	False	False
	zero_tracer_source	False	False	False
ocean_velocity_diag_nml	debug_this_module	False	False	False
	diag_step	4320	4320	576
	energy_diag_step	4320	4320	5760
	large_cfl_value	10.0	10.0	10.0
	max_cfl_value	100.0	100.0	100.0
ocean_velocity_nml	adams_bashforth_third	True	True	True

Group (continued)	Variable	/short/ v45/ amh157/ access- om2/ control/ 1deg- jra55_ryf/ ocean/ input.nml	/short/ v45/ aek156/ access- om2/ control/ 025deg- jra55_ryf/ ocean/ input.nml	/short/ v45/ amh157/ access- om2/ control/ 01deg- jra55_ryf/ ocean/ input.nml
	max_cgint	1.0	1.5	1.0
	truncate_velocity	True	False	False
	truncate_velocity_value	2.0	2.0	2.0
	truncate_verbose	True	True	True
	zero_tendency	False	False	False
	zero_tendency_explicit_a		False	False
	zero_tendency_explicit_b		False	False
	zero_tendency_implicit		False	False
ocean_vert_kpp_iow_nml	use_this_module	False	False	False
ocean_vert_kpp_mom4p0_nml	use_this_module	False		
ocean_vert_kpp_mom4p1_nml	diff_cbt_iw	0.0	0.0	0.0
	diff_con_limit	0.1		
	double_diffusion	True	True	True
	kbl_standard_method	False	False	False
	ricr	0.3	0.3	0.3
	smooth_blmc	False	False	False
	smooth_ri_kmax_eq_kmu	True	True	True
	use_this_module	True	True	True
	visc_cbu_iw	0.0	0.0	0.0
	visc_con_limit	0.1		
ocean_vert_mix_nml	afkph_00	0.65		
	afkph_90	0.75		
	aidif	1.0	1.0	1.0
	bryan_lewis_diffusivity	False	False	False
	bryan_lewis_lat_depend	True	False	False
	bryan_lewis_lat_transition	35.0		
	dfkph_00	1.15		
	dfkph_90	0.95		
	hwf_diffusivity		False	False
	hwf_min_diffusivity		2×10^{-6}	2×10^{-6}
	hwf_n0_2omega		20.0	20.0
	linear_taper_diff_cbt_table	False		
	sfkph_00	4.5×10^{-5}		
	sfkph_90	4.5×10^{-5}		
	use_diff_cbt_table	False	False	False
	vert_diff_back_via_max	True	True	True
	vert_mix_scheme	'kpp- mom4p1'	'kpp- mom4p1'	'kpp- mom4p1'
	zfkph_00	250 000.0		
	zfkph_90	250 000.0		
ocean_vert_tidal_nml	background_diffusivity	5×10^{-6}	0.0	0.0
	background_viscosity	0.0001	0.0001	0.0001
	decay_scale	300.0	500.0	500.0
	drag_dissipation_use_cdbot		True	True
	drhodz_min	1×10^{-12}	1×10^{-10}	1×10^{-10}
	fixed_wave_dissipation	False	False	False
	max_drag_diffusivity	0.01		

Group (continued)	Variable	/short/ v45/ amh157/ access- om2/ control/ 1deg_- jra55_ryf/ ocean/ input.nml	/short/ v45/ aek156/ access- om2/ control/ 025deg_- jra55_ryf/ ocean/ input.nml	/short/ v45/ amh157/ access- om2/ control/ 01deg_- jra55_ryf/ ocean/ input.nml
	max_wave_diffusivity	0.01	0.01	0.01
	mixing_efficiency_n2depend	True	True	True
	read_roughness	True	True	True
	read_tide_speed	True	True	True
	read_wave_dissipation	False	False	False
	reading_roughness_amp	True	True	True
	reading_roughness_length	False	False	False
	roughness_scale	20 000.0	12 000.0	12 000.0
	shelf_depth_cutoff	160.0	—1000.0	—1000.0
	tide_speed_data_on_t_grid	True	True	True
	use_drag_dissipation	True	True	True
	use_legacy_methods		False	False
	use_this_module	True	True	True
	use_wave_dissipation	True	True	True
	wave_energy_flux_max	0.1	0.1	0.1
ocean_xlandinsert.nml	use_this_module	False	False	False
	verbose_init	True		
ocean_xlandmix.nml	use_this_module	False	False	False
	verbose_init	True		
	xlandmix_kmt	True		
sat_vapor_pres.nml	show_all_bad_values			True
surface_flux.nml	ncar_ocean_flux		True	True
	raoult_sat_vap		True	True
xgrid.nml	do_alltoall			True
	do_alltoallv			True
	interp_method	'second_- order'	'second_- order'	'second_- order'
	make_exchange_reproduce	False	False	False
	nsubset		16	16
	xgrid_log			False

A.2 CICE namelists

A.2.1 cice.in.nml

Group	Variable	/short/ v45/ amh157/ access- om2/ control/ 1deg_- jra55_ryf/ ice/cice_- in.nml	/short/ v45/ aek156/ access- om2/ control/ 025deg_- jra55_ryf/ ice/cice_- in.nml	/short/ v45/ amh157/ access- om2/ control/ 01deg_- jra55_ryf/ ice/cice_- in.nml
domain.nml	distribution_type	'cartesian'	'cartesian'	'cartesian'
	distribution_wght	'latitude'	'latitude'	'latitude'
	ew_boundary_type	'cyclic'	'cyclic'	'cyclic'
	maskhalo_bound	True	True	True
	maskhalo_dyn	True	True	True

Group (continued)	Variable	/short/ v45/ amh157/ access- om2/ control/ 1deg_- jra55_ryf/ ice/cice_- in.nml	/short/ v45/ aek156/ access- om2/ control/ 025deg_- jra55_ryf/ ice/cice_- in.nml	/short/ v45/ amh157/ access- om2/ control/ 01deg_- jra55_ryf/ ice/cice_- in.nml
	maskhalo_remap	True	True	True
	nprocs	24	480	1200
	ns_boundary_type	'tripole'	'tripole'	'tripole'
	processor_shape	'slenderX1'	'square-ice'	'square-ice'
dynamics_nml	advection	'remap'	'remap'	'remap'
	cosw	0.96	0.96	0.96
	dragio	0.005 36	0.005 36	0.005 36
	iceruf	0.0005	0.0005	0.0005
	kdyn	1	1	1
	krdg_partic	1	1	1
	krdg_redist	1	1	1
	kstrength	1	1	1
	mu_rdg	3	3	3
	ndte	120	120	120
	revised_evp	False	False	False
	sinw	0.28	0.28	0.28
forcing_nml	atm_data_dir	'unknown_- atm_- data_dir'	'unknown_- atm_- data_dir'	'unknown_- atm_- data_dir'
	atm_data_format	'nc'	'nc'	'nc'
	atm_data_type	'default'	'default'	'default'
	atmbndy	'default'	'default'	'default'
	calc_strair	True	True	True
	calc_tsfc	True	True	True
	formdrag	False	False	False
	fyear_init	1	1	1
	oceanmixed_file	'unknown_- ocean- mixed_file'	'unknown_- ocean- mixed_file'	'unknown_- ocean- mixed_file'
	oceanmixed_ice	False	False	False
	ocn_data_dir	'unknown_- ocn_data_- dir'	'unknown_- ocn_data_- dir'	'unknown_- ocn_data_- dir'
	ocn_data_format	'nc'	'nc'	'nc'
	precip_units	'mks'	'mks'	'mks'
	restore_ice	False	False	False
	restore_sst	False	False	False
	sss_data_type	'default'	'default'	'default'
	sst_data_type	'default'	'default'	'default'
	trestore	0	0	0
	update_ocn_f	True	True	True
	ustar_min	0.0005	0.0005	0.0005
	ycycle	1	1	1
grid_nml	grid_file	'RESTART/ grid.nc'	'RESTART/ grid.nc'	'RESTART/ grid.nc'
	grid_format	'nc'	'nc'	'nc'
	grid_type	'tripole'	'tripole'	'tripole'
	kcatbound	0	0	0
	kmt_file	'RESTART/ kmt.nc'	'RESTART/ kmt.nc'	'RESTART/ kmt.nc'
icefields_bgc_nml	f_aero	'x'	'x'	'x'

Group (continued)	Variable	/short/ v45/ amh157/ access- om2/ control/ 1deg_- jra55_ryf/ ice/cice_- in.nml	/short/ v45/ aek156/ access- om2/ control/ 025deg_- jra55_ryf/ ice/cice_- in.nml	/short/ v45/ amh157/ access- om2/ control/ 01deg_- jra55_ryf/ ice/cice_- in.nml
	f_bgc_am_ml	'x'	'x'	'x'
	f_bgc_am_sk	'x'	'x'	'x'
	f_bgc_c_sk	'x'	'x'	'x'
	f_bgc_chl_sk	'x'	'x'	'x'
	f_bgc_dms_sk	'x'	'x'	'x'
	f_bgc_dmsp_ml	'x'	'x'	'x'
	f_bgc_dmspd_sk	'x'	'x'	'x'
	f_bgc_dmspp_sk	'x'	'x'	'x'
	f_bgc_n_sk	'x'	'x'	'x'
	f_bgc_nit_ml	'x'	'x'	'x'
	f_bgc_nit_sk	'x'	'x'	'x'
	f_bgc_sil_ml	'x'	'x'	'x'
	f_bgc_sil_sk	'x'	'x'	'x'
	f_bphi	'x'	'x'	'x'
	f_btin	'x'	'x'	'x'
	f_faero_atm	'x'	'x'	'x'
	f_faero_ocn	'x'	'x'	'x'
	f_fbri	'm'	'm'	'x'
	f_fn	'x'	'x'	'x'
	f_fn_ai	'x'	'x'	'x'
	f_fnh	'x'	'x'	'x'
	f_fnh_ai	'x'	'x'	'x'
	f_fno	'x'	'x'	'x'
	f_fno_ai	'x'	'x'	'x'
	f_fsil	'x'	'x'	'x'
	f_fsil_ai	'x'	'x'	'x'
	f_grownet	'x'	'x'	'x'
	f_hbri	'm'	'm'	'x'
	f_ppnet	'x'	'x'	'x'
icefields_drag_nml	f_cdn_atm	'x'	'x'	'x'
	f_cdn_ocn	'x'	'x'	'x'
	f_drag	'x'	'x'	'x'
icefields_mechred_nml	f_alvl	'm'	'm'	'x'
	f_aparticn	'x'	'x'	'x'
	f_araftn	'x'	'x'	'x'
	f_ardg	'm'	'm'	'x'
	f_ardgn	'x'	'x'	'x'
	f_aredistn	'x'	'x'	'x'
	f_dardg1dt	'x'	'x'	'x'
	f_dardg1ndt	'x'	'x'	'x'
	f_dardg2dt	'x'	'x'	'x'
	f_dardg2ndt	'x'	'x'	'x'
	f_dvirdgdt	'x'	'x'	'x'
	f_dvirdgndt	'x'	'x'	'x'
	f_krdgn	'x'	'x'	'x'
	f_opening	'x'	'x'	'x'
	f_vlvl	'm'	'm'	'x'
	f_vraftn	'x'	'x'	'x'
	f_vrdg	'm'	'm'	'x'
	f_vrdgn	'x'	'x'	'x'

Group (continued)	Variable	/short/ v45/ amh157/ access- om2/ control/ 1deg_- jra55_ryf/ ice/cice_- in.nml	/short/ v45/ aek156/ access- om2/ control/ 025deg_- jra55_ryf/ ice/cice_- in.nml	/short/ v45/ amh157/ access- om2/ control/ 01deg_- jra55_ryf/ ice/cice_- in.nml
	f_vredistn	'x'	'x'	'x'
icefields_nml	f_aice	'm'	'm'	'm'
	f_aicen	'm'	'm'	'x'
	f_aisnap	'x'	'x'	'x'
	f_albice	'm'	'm'	'x'
	f_albpnd	'x'	'x'	'x'
	f_albsni	'm'	'm'	'x'
	f_albsno	'm'	'm'	'x'
	f_alidr	'x'	'x'	'x'
	f_alvdr	'x'	'x'	'x'
	f_angle	True	True	True
	f_anglet	True	True	True
	f_bounds	False	False	False
	f_congel	'm'	'm'	'x'
	f_coszen	'x'	'x'	'x'
	f_daidd	'm'	'm'	'x'
	f_daiddt	'm'	'm'	'x'
	f_divu	'm'	'm'	'x'
	f_dsnw	'x'	'x'	'x'
	f_dvidtd	'm'	'm'	'x'
	f_dvidtt	'm'	'm'	'x'
	f_dxt	True	True	True
	f_dxu	True	True	True
	f_dyt	True	True	True
	f_dyu	True	True	True
	f_evap	'x'	'x'	'x'
	f_evap_ai	'm'	'm'	'x'
	f_fcondtop_ai	'm'	'm'	'x'
	f_fcondtopn_ai	'm'	'm'	'x'
	f_fhocn	'x'	'x'	'x'
	f_fhocn_ai	'm'	'm'	'x'
	f_flat	'x'	'x'	'x'
	f_flat_ai	'm'	'm'	'x'
	f_flatn_ai	'm'	'm'	'x'
	f_flwdn	'm'	'm'	'x'
	f_flwup	'x'	'x'	'x'
	f_flwup_ai	'm'	'm'	'x'
	f_fmeltt_ai	'x'	'x'	'x'
	f_fmelttn_ai	'm'	'm'	'x'
	f_frazil	'm'	'm'	'x'
	f_fresh	'x'	'x'	'x'
	f_fresh_ai	'm'	'm'	'x'
	f_frz_onset	'm'	'm'	'x'
	f_frzmlt	'm'	'm'	'x'
	f_fsalt	'x'	'x'	'x'
	f_fsalt_ai	'm'	'm'	'x'
	f_fsens	'x'	'x'	'x'
	f_fsens_ai	'm'	'm'	'x'
	f_fsurf_ai	'x'	'x'	'x'
	f_fsurfn_ai	'm'	'm'	'x'
	f_fswabs	'x'	'x'	'x'

Group (continued)	Variable	/short/ v45/ amh157/ access- om2/ control/ 1deg_- jra55_ryf/ ice/cice_- in.nml	/short/ v45/ aek156/ access- om2/ control/ 025deg_- jra55_ryf/ ice/cice_- in.nml	/short/ v45/ amh157/ access- om2/ control/ 01deg_- jra55_ryf/ ice/cice_- in.nml
	f_fswabs_ai	'm'	'm'	'x'
	f_fswdn	'm'	'm'	'x'
	f_fswfac	'm'	'm'	'x'
	f_fswthru	'x'	'x'	'x'
	f_fswthru_ai	'm'	'm'	'x'
	f_fy	'x'	'x'	'x'
	f_hi	'm'	'm'	'm'
	f_hisnap	'x'	'x'	'x'
	f_hs	'm'	'm'	'm'
	f_hte	True	True	True
	f_htn	True	True	True
	f_iage	'm'	'm'	'x'
	f_icepresent	'm'	'm'	'x'
	f_meltb	'm'	'm'	'x'
	f_meltl	'm'	'm'	'x'
	f_melts	'm'	'm'	'x'
	f_meltt	'm'	'm'	'x'
	f_mlt_onset	'm'	'm'	'x'
	f_ncat	True	True	True
	f_qref	'x'	'x'	'x'
	f_rain	'x'	'x'	'x'
	f_rain_ai	'm'	'm'	'x'
	f_shear	'm'	'm'	'x'
	f_sice	'm'	'm'	'x'
	f_sig1	'x'	'x'	'x'
	f_sig2	'x'	'x'	'x'
	f_sinz	'x'	'x'	'x'
	f_snoice	'm'	'm'	'x'
	f_snow	'x'	'x'	'x'
	f_snow_ai	'm'	'm'	'x'
	f_sss	'm'	'm'	'x'
	f_sst	'm'	'm'	'x'
	f_strairx	'm'	'm'	'x'
	f_strairy	'm'	'm'	'x'
	f_strcorx	'm'	'm'	'x'
	f_strcory	'm'	'm'	'x'
	f_strength	'm'	'm'	'x'
	f_strintx	'm'	'm'	'x'
	f_strinty	'm'	'm'	'x'
	f_strocnx	'm'	'm'	'x'
	f_strocny	'm'	'm'	'x'
	f_strltlx	'm'	'm'	'x'
	f_strltly	'm'	'm'	'x'
	f_tair	'm'	'm'	'x'
	f_tarea	True	True	True
	f_tinz	'x'	'x'	'x'
	f_tmask	True	True	True
	f_tref	'x'	'x'	'x'
	f_trsig	'm'	'm'	'x'
	f_tsfc	'm'	'm'	'm'
	f_tsnz	'x'	'x'	'x'

Group (continued)	Variable	/short/ v45/ amh157/ access- om2/ control/ 1deg_- jra55_ryf/ ice/cice_- in.nml	/short/ v45/ aek156/ access- om2/ control/ 025deg_- jra55_ryf/ ice/cice_- in.nml	/short/ v45/ amh157/ access- om2/ control/ 01deg_- jra55_ryf/ ice/cice_- in.nml
	f_uarea	True	True	True
	f_uocn	'm'	'm'	'x'
	f_uvel	'm'	'm'	'x'
	f_vgrdb	False	False	False
	f_vgrdi	False	False	False
	f_vgrds	False	False	False
	f_vicen	'm'	'm'	'x'
	f_vocn	'm'	'm'	'x'
	f_vvel	'm'	'm'	'x'
icefields_pond.nml	f_apeff	'm'	'm'	'x'
	f_apeff_ai	'm'	'm'	'x'
	f_apeffn	'x'	'x'	'x'
	f_apon	'm'	'm'	'x'
	f_apon_ai	'm'	'm'	'x'
	f_apon	'x'	'x'	'x'
	f_hpond	'm'	'm'	'x'
	f_hpond_ai	'm'	'm'	'x'
	f_hpondn	'x'	'x'	'x'
	f_ipond	'm'	'm'	'x'
	f_ipond_ai	'm'	'm'	'x'
ponds.nml	dpscale	0.001	0.001	0.001
	frzpond	'hlid'	'hlid'	'hlid'
	hp1	0.01	0.01	0.01
	hs0	0.0	0.0	0.0
	hs1	0.03	0.03	0.03
	pndaspect	0.8	0.8	0.8
	rfracmax	1.0	1.0	1.0
	rfracmin	0.15	0.15	0.15
setup.nml	days_per_year	365	365	365
	debug	False	False	False
	diag_file	'ice_diag.d'	'ice_diag.d'	'ice_diag.d'
	diag_type	'file'	'file'	'file'
	diagfreq	24	960	960
	dt	3600	1200	400
	dump_last	True	True	True
	dumpfreq	'y'	'y'	'm'
	dumpfreq_n	1	1	3
	hist_avg	True	True	True
	histfreq	'd', 'm', 'x', 'x', 'x'	'd', 'm', 'x', 'x', 'x'	'd', 'm', 'x', 'x', 'x'
	histfreq_n	1, 1, 1, 1, 1	1, 1, 1, 1, 1	1, 1, 1, 1, 1
	history_dir	'./OUTPUT/',	'./OUTPUT/',	'./OUTPUT/',
	history_file	'iceh'	'iceh'	'iceh'
	ice_ic	'default'	'default'	'default'
	incond_dir	'./OUTPUT/',	'./OUTPUT/',	'./OUTPUT/',
	incond_file	'iceh_ic'	'iceh_ic'	'iceh_ic'
	istep0	0	0	0
	latpnt	90.0, -65.0	90.0, -65.0	90.0, -65.0

Group (continued)	Variable	/short/ v45/ amh157/ access- om2/ control/ 1deg_- jra55_ryf/ ice/cice_- in.nml	/short/ v45/ aek156/ access- om2/ control/ 025deg_- jra55_ryf/ ice/cice_- in.nml	/short/ v45/ amh157/ access- om2/ control/ 01deg_- jra55_ryf/ ice/cice_- in.nml
	lcdf64	False	True	True
	lonpnt	0.0, -45.0	0.0, -45.0	0.0, -45.0
	ndtd	1	1	1
	npt	35040	2232	6480
	pointer_file	./	./	./
		RESTART/ ice.restart_- file'	RESTART/ ice.restart_- file'	RESTART/ ice.restart_- file'
	print_global	False	False	False
	print_points	False	False	False
	restart	False	False	False
	restart_dir	./	./	./
		RESTART/'	RESTART/'	RESTART/'
	restart_ext	False	False	False
	restart_file	'iced'	'iced'	'iced'
	restart_format	'nc'	'nc'	'nc'
	runtype	'initial'	'initial'	'initial'
	use_leap_years	False	False	False
	use_restart_time	True	True	True
	write_ic	False	False	False
	year_init	1	1	1
shortwave_nml	ahmax	0.1	0.1	0.1
	albedo_type	'default'	'default'	'default'
	albice_i	0.44	0.44	0.44
	albice_v	0.86	0.86	0.86
	albsnow_i	0.7	0.7	0.7
	albsnow_v	0.98	0.98	0.98
	dalb_mlt	-0.02	-0.02	-0.02
	dt_mlt	1.0	1.0	1.0
	r_ice	0.0	0.0	0.0
	r_pnd	0.0	0.0	0.0
	r_snw	0.0	0.0	0.0
	rsnw_mlt	1500.0	1500.0	1500.0
	shortwave	'default'	'default'	'default'
	tocnfrz	-1.8	-1.8	-1.8
thermo_nml	a_rapid_mode	0.0005	0.0005	0.0005
	aspect_rapid_mode	1.0	1.0	1.0
	chio	0.004	0.004	0.004
	conduct	'bubbly'	'bubbly'	'bubbly'
	dsdt_slow_mode	-5 × 10 ⁻⁸	-5 × 10 ⁻⁸	-5 × 10 ⁻⁸
	kitd	1	1	1
	ktherm	1	1	1
	phi_c_slow_mode	0.05	0.05	0.05
	phi_i_mushy	0.85	0.85	0.85
	rac_rapid_mode	10.0	10.0	10.0
tracer_nml	restart_aero	False	False	False
	restart_age	False	False	False
	restart_fy	False	False	False
	restart_lvl	False	False	False
	restart_pond_cesm	False	False	False

Group (continued)	Variable	/short/ v45/ amh157/ access- om2/ control/ 1deg_- jra55_ryf/ ice/cice_- in.nml	/short/ v45/ aek156/ access- om2/ control/ 025deg_- jra55_ryf/ ice/cice_- in.nml	/short/ v45/ amh157/ access- om2/ control/ 01deg_- jra55_ryf/ ice/cice_- in.nml
	restart_pond_lvl	False	False	False
	restart_pond_topo	False	False	False
	tr_aero	False	False	False
	tr_fy	False	False	False
	tr_iage	False	False	False
	tr_lvl	False	False	False
	tr_pond_cesm	False	False	False
	tr_pond_lvl	False	False	False
	tr_pond_topo	False	False	False
zbgc_nml	bgc_data_dir	'unknown_- bgc_data_- dir'	'unknown_- bgc_data_- dir'	'unknown_- bgc_data_- dir'
	bgc_flux_type	'Jin2006'	'Jin2006'	'Jin2006'
	nit_data_type	'default'	'default'	'default'
	phi_snow	0.5	0.5	0.5
	restart_bgc	False	False	False
	restart_hbrine	False	False	False
	restore_bgc	False	False	False
	sil_data_type	'default'	'default'	'default'
	skl_bgc	False	False	False
	tr_bgc_am_sk	False	False	False
	tr_bgc_c_sk	False	False	False
	tr_bgc_chl_sk	False	False	False
	tr_bgc_dms_sk	False	False	False
	tr_bgc_dmspd_sk	False	False	False
	tr_bgc_dmspp_sk	False	False	False
	tr_bgc_sil_sk	False	False	False
	tr_brine	False	False	False

A.2.2 input_ice.nml

Group	Variable	/short/ v45/ amh157/ access- om2/ control/ 1deg_- jra55_ryf/ ice/ input_- ice.nml	/short/ v45/ aek156/ access- om2/ control/ 025deg_- jra55_ryf/ ice/ input_- ice.nml	/short/ v45/ amh157/ access- om2/ control/ 01deg_- jra55_ryf/ ice/ input_- ice.nml
coupling_nml	chk_a2i_fields	False	False	False
	chk_frzmlt_sst		False	False
	chk_gfdl_roughness	False	False	False
	chk_i2a_fields		False	False
	chk_i2o_fields		False	False
	chk_o2i_fields		False	False
	cst_ocn_albedo	True	True	True

Group (continued)	Variable	/short/ v45/ amh157/ access- om2/ control/ 1deg_- jra55_ryf/ ice/ input_- ice.nml	/short/ v45/ aek156/ access- om2/ control/ 025deg_- jra55_ryf/ ice/ input_- ice.nml	/short/ v45/ amh157/ access- om2/ control/ 01deg_- jra55_ryf/ ice/ input_- ice.nml
	dt_cpl_ai	10800	10800	10800
	dt_cpl_io	3600	1200	400
	gfdl_surface_flux	True	True	True
	ice_fwflux	True	True	True
	ice_pressure_on	True	True	True
	limit_icemelt	False	False	False
	meltlimit	−200.0	−200.0	−200.0
	ocn_albedo	0.1	0.1	0.1
	pop_icediag	True	True	True
	precip_factor	1.0	1.0	1.0
	rotate_winds	True	True	True
	use_ocnslope	False	False	False
	use_umask	False	False	False

A.2.3 input_ice_gfdl.nml

Group	Variable	/short/ v45/ amh157/ access- om2/ control/ 1deg_- jra55_ryf/ ice/ input_- ice_- gfdl.nml	/short/ v45/ aek156/ access- om2/ control/ 025deg_- jra55_ryf/ ice/ input_- ice_- gfdl.nml	/short/ v45/ amh157/ access- om2/ control/ 01deg_- jra55_ryf/ ice/ input_- ice_- gfdl.nml
ocean_rough.nml	charnock	0.032	0.032	0.032
	do_cap40	False	False	False
	do_highwind	False	False	False
	rough_scheme	'beljaars'	'beljaars'	'beljaars'
	roughness_heat	5.8×10^{-5}	5.8×10^{-5}	5.8×10^{-5}
	roughness_min	1×10^{-6}	1×10^{-6}	1×10^{-6}
	roughness_moist	5.8×10^{-5}	5.8×10^{-5}	5.8×10^{-5}
	roughness_mom	5.8×10^{-5}	5.8×10^{-5}	5.8×10^{-5}
	zcoh1	0.0	0.0	0.0
	zcoq1	0.0	0.0	0.0
surface_flux.nml	alt_gustiness	False	False	False
	gust_const	1.0	1.0	1.0
	gust_min	0.0	0.0	0.0
	ncar_ocean_flux	True	True	True
	ncar_ocean_flux_orig	False	False	False
	no_neg_q	False	False	False
	old_dtaudv	False	False	False

Group (continued)	Variable	/short/ v45/ amh157/ access- om2/ control/ 1deg_- jra55_ryf/ ice/ input_- ice_- gfdl.nml	/short/ v45/ aek156/ access- om2/ control/ 025deg_- jra55_ryf/ ice/ input_- ice_- gfdl.nml	/short/ v45/ amh157/ access- om2/ control/ 01deg_- jra55_ryf/ ice/ input_- ice_- gfdl.nml
	raoult_sat_vap	False	False	False
	use_mixing_ratio	False	False	False
	use_virtual_temp	True	True	True

A.2.4 input_ice_monin.nml

Group	Variable	/short/ v45/ amh157/ access- om2/ control/ 1deg_- jra55_ryf/ ice/ input_- ice_- monin.nml	/short/ v45/ aek156/ access- om2/ control/ 025deg_- jra55_ryf/ ice/ input_- ice_- monin.nml	/short/ v45/ amh157/ access- om2/ control/ 01deg_- jra55_ryf/ ice/ input_- ice_- monin.nml
monin_obukhov.nml	neutral	True	True	True

A.3 MATM namelist 'input_atm.nml'

Group	Variable	/short/ v45/ amh157/ access- om2/ control/ 1deg_- jra55_ryf/ atmosphere, input_- atm.nml	/short/ v45/ aek156/ access- om2/ control/ 025deg_- jra55_ryf/ atmosphere, input_- atm.nml	/short/ v45/ amh157/ access- om2/ control/ 01deg_- jra55_ryf/ atmosphere/ input_- atm.nml
coupling	caltype	0	0	0
	chk_a2i_fields	False	False	
	chk_i2a_fields	False	False	
	dataset	'jra55'	'jra55'	'jra55'
	days_per_year	365	365	365
	debug_output	False		
	dt_atm	3600	1200	400
	dt_cpl	10800	10800	10800
	inidate	10101	10101	10101
	init_date	10101	10101	10101
	runtime	126144000	2678400	2592000
	runtype	'NY'	'NY'	'NY'
	truntime0	0	0	0

B Auto-generated tables of namelist changes within runs

C Auto-generated tables of namelist differences from ACCESS, ACCESS-CM2, ACCESS-ESM, OFAM

C.1 ACCESS-OM2-01 MOM compared to OFAM3

C.2 ACCESS-OM2-01 MOM compared to MOM-SIS-01 and GFDL

C.3 ACCESS-OM2-01 CICE compared to RASM and NCAR

ice_in_RASM [TODO: get permission](#)

ncar_ice_in [TODO: get permission](#)

References

- Abernathey, R. P., I. Cerovecki, P. R. Holland, E. Newsom, M. Mazloff, and L. D. Talley, 2016: Water-mass transformation by sea ice in the upper branch of the Southern Ocean overturning. *Nature Geoscience*, **9** (8), 596–601, doi:10.1038/ngeo2749, URL <http://dx.doi.org/10.1038/ngeo2749>.
- Archer, M., M. Roughan, S. Keating, and A. Schaeffer, 2017a: On the variability of the East Australian Current: Jet structure, meandering, and influence on shelf circulation. *Journal of Geophysical Research: Oceans*, doi:10.1002/2017jc013097, URL <http://dx.doi.org/10.1002/2017JC013097>.
- Archer, M. R., S. R. Keating, M. Roughan, W. E. Johns, R. Lumpkin, F. Beron-Vera, and L. K. Shay, 2018: The kinematic similarity of two western boundary currents revealed by sustained high-resolution observations. *Geophysical Research Letters*, doi:10.1029/2018gl078429, URL <http://dx.doi.org/10.1029/2018GL078429>.
- Archer, M. R., L. K. Shay, and W. E. Johns, 2017b: The surface velocity structure of the Florida Current in a jet coordinate frame. *Journal of Geophysical Research: Oceans*, doi:10.1002/2017jc013286, URL <http://dx.doi.org/10.1002/2017JC013286>.
- Bamber, J., M. van den Broeke, J. Ettema, J. Lenaerts, and E. Rignot, 2012: Recent large increases in freshwater fluxes from Greenland into the North Atlantic. *Geophysical Research Letters*, **39** (19), n/a–n/a, doi:10.1029/2012gl052552, URL <http://dx.doi.org/10.1029/2012GL052552>.
- Bi, D., H. Yan, and A. Sullivan, 2016: ACCESS-CM2 development. *COSIMA workshop 26-27 May 2016, Hobart*, URL <http://cosima.org.au/wp-content/uploads/2016/06/BI-COSIMA-Hobart-20160526.ppt.pdf>.
- Bi, D., and Coauthors, 2013a: The ACCESS coupled model: description, control climate and evaluation. *Australian Meteorological and Oceanographic Journal*, **63** (1), 41–64.
- Bi, D., and Coauthors, 2013b: ACCESS-OM: the ocean and sea-ice core of the ACCESS coupled model. *Australian Meteorological and Oceanographic Journal*, **63** (1), 213–232.
- Bouillon, S., T. Fichefet, V. Legat, and G. Madec, 2013: The elastic–viscous–plastic method revisited. *Ocean Modelling*, **71**, 2–12, doi:10.1016/j.ocemod.2013.05.013, URL <http://dx.doi.org/10.1016/j.ocemod.2013.05.013>.
- Capet, X., J. C. McWilliams, M. J. Molemaker, and A. F. Shchepetkin, 2008: Mesoscale to submesoscale transition in the California Current system. Part I: Flow structure, eddy flux, and observational tests. *Journal of Physical Oceanography*, **38** (1), 29–43, doi:10.1175/2007JPO3671.1, URL <http://dx.doi.org/10.1175/2007JPO3671.1>.

- Cassano, J. J., and Coauthors, 2017: Development of the Regional Arctic System Model (RASM): Near-surface atmospheric climate sensitivity. *Journal of Climate*, **30** (15), 5729–5753, doi:10.1175/jcli-d-15-0775.1, URL <http://dx.doi.org/10.1175/JCLI-D-15-0775.1>.
- Colin de Verdière, A., and M. Ollitrault, 2016: A direct determination of the world ocean barotropic circulation. *Journal of Physical Oceanography*, **46** (1), 255–273, doi:10.1175/jpo-d-15-0046.1, URL <http://dx.doi.org/10.1175/JPO-D-15-0046.1>.
- Craig, A. P., S. A. Mickelson, E. C. Hunke, and D. A. Bailey, 2014: Improved parallel performance of the CICE model in CESM1. *The International Journal of High Performance Computing Applications*, **29** (2), 154–165, doi:10.1177/1094342014548771, URL <http://dx.doi.org/10.1177/1094342014548771>.
- Danabasoglu, G., and Coauthors, 2014: North Atlantic simulations in Coordinated Ocean-ice Reference Experiments phase II (CORE-II). Part I: Mean states. *Ocean Modelling*, **73**, 76–107, doi:10.1016/j.ocemod.2013.10.005, URL <http://dx.doi.org/10.1016/j.ocemod.2013.10.005>.
- Danabasoglu, G., and Coauthors, 2016: North Atlantic simulations in Coordinated Ocean-ice Reference Experiments phase II (CORE-II). Part II: Inter-annual to decadal variability. *Ocean Modelling*, **97**, 65–90, doi:10.1016/j.ocemod.2015.11.007, URL <http://dx.doi.org/10.1016/j.ocemod.2015.11.007>.
- Dansereau, V., J. Weiss, P. Saramito, and P. Lattes, 2016: A Maxwell elasto-brittle rheology for sea ice modelling. *The Cryosphere*, **10** (3), 1339–1359, doi:10.5194/tc-10-1339-2016, URL <http://dx.doi.org/10.5194/tc-10-1339-2016>.
- Delworth, T. L., and Coauthors, 2012: Simulated climate and climate change in the GFDL CM2.5 high-resolution coupled climate model. *Journal of Climate*, **25** (8), 2755–2781, doi:10.1175/jcli-d-11-00316.1, URL <http://dx.doi.org/10.1175/JCLI-D-11-00316.1>.
- Depoorter, M. A., J. L. Bamber, J. A. Griggs, J. T. M. Lenaerts, S. R. M. Ligtenberg, M. R. van den Broeke, and G. Moholdt, 2013: Calving fluxes and basal melt rates of Antarctic ice shelves. *Nature*, **502** (7469), 89–92, doi:10.1038/nature12567, URL <http://dx.doi.org/10.1038/nature12567>.
- Dix, M., and Coauthors, 2013: The ACCESS coupled model: Documentation of core CMIP5 simulations and initial results. *Australian Meteorological and Oceanographic Journal*, **63** (1), 83–99.
- Donat-Magnin, M., N. C. Jourdain, P. Spence, J. Le Sommer, H. Gallée, and G. Durand, 2017: Ice-shelf melt response to changing winds and glacier dynamics in the amundsen sea sector, antarctica. *Journal of Geophysical Research: Oceans*, **122** (12), 10 206–10 224, doi:10.1002/2017jc013059, URL <http://dx.doi.org/10.1002/2017JC013059>.
- Donohue, K. A., K. L. Tracey, D. R. Watts, M. P. Chidichimo, and T. K. Chereskin, 2016: Mean Antarctic Circumpolar Current transport measured in Drake Passage. *Geophysical Research Letters*, **43** (22), 11,760–11,767, doi:10.1002/2016gl070319, URL <http://dx.doi.org/10.1002/2016GL070319>.
- Downes, S. M., A. Gnanadesikan, S. M. Griffies, and J. L. Sarmiento, 2011: Water mass exchange in the Southern Ocean in coupled climate models. *Journal of Physical Oceanography*, **41** (9), 1756–1771, doi:10.1175/2011jpo4586.1, URL <http://dx.doi.org/10.1175/2011JPO4586.1>.
- Downes, S. M., and Coauthors, 2015: An assessment of Southern Ocean water masses and sea ice during 1988–2007 in a suite of interannual CORE-II simulations. *Ocean Modelling*, **94**, 67–94, doi:10.1016/j.ocemod.2015.07.022, URL <http://dx.doi.org/10.1016/j.ocemod.2015.07.022>.
- Dunne, J. P., and Coauthors, 2012: GFDL’s ESM2 global coupled climate–carbon earth system models. Part I: Physical formulation and baseline simulation characteristics. *Journal of Climate*, **25** (19), 6646–6665, doi:10.1175/jcli-d-11-00560.1, URL <http://dx.doi.org/10.1175/JCLI-D-11-00560.1>.

- Farneti, R., and Coauthors, 2015: An assessment of Antarctic Circumpolar Current and Southern Ocean meridional overturning circulation during 1958–2007 in a suite of interannual CORE-II simulations. *Ocean Modelling*, **93**, 84–120, doi:10.1016/j.ocemod.2015.07.009, URL <http://dx.doi.org/10.1016/j.ocemod.2015.07.009>.
- Girard, L., J. Weiss, J. M. Molines, B. Barnier, and S. Bouillon, 2009: Evaluation of high-resolution sea ice models on the basis of statistical and scaling properties of Arctic sea ice drift and deformation. *Journal of Geophysical Research*, **114** (C8), doi:10.1029/2008jc005182, URL <http://dx.doi.org/10.1029/2008JC005182>.
- Gregory, J. M., and Coauthors, 2016: The flux-anomaly-forced model intercomparison project (FAFMIP) contribution to CMIP6: investigation of sea-level and ocean climate change in response to CO₂ forcing. *Geoscientific Model Development*, **9** (11), 3993–4017, doi:10.5194/gmd-9-3993-2016, URL <http://dx.doi.org/10.5194/gmd-9-3993-2016>.
- Griffies, S., 2015: A handbook for the GFDL CM2-O model suite. Technical Report 1, GFDL Climate Processes and Sensitivity Group, NOAA/GFDL Princeton, USA.
- Griffies, S. M., 2012: Elements of the Modular Ocean Model (MOM) 5 (2012 release). Technical Report 7, NOAA/Geophysical Fluid Dynamics Laboratory Ocean Group.
- Griffies, S. M., and Coauthors, 2009: Coordinated ocean-ice reference experiments (COREs). *Ocean Modelling*, **26** (1–2), 1–46, doi:10.1016/j.ocemod.2008.08.007, URL <http://dx.doi.org/10.1016/j.ocemod.2008.08.007>.
- Griffies, S. M., and Coauthors, 2014: An assessment of global and regional sea level for years 1993–2007 in a suite of interannual CORE-II simulations. *Ocean Modelling*, **78**, 35–89, doi:10.1016/j.ocemod.2014.03.004, URL <http://dx.doi.org/10.1016/j.ocemod.2014.03.004>.
- Griffies, S. M., and Coauthors, 2015: Impacts on ocean heat from transient mesoscale eddies in a hierarchy of climate models. *Journal of Climate*, **28** (3), 952–977, doi:10.1175/jcli-d-14-00353.1, URL <http://dx.doi.org/10.1175/JCLI-D-14-00353.1>.
- Griffies, S. M., and Coauthors, 2016: OMIP contribution to CMIP6: experimental and diagnostic protocol for the physical component of the Ocean Model Intercomparison Project. *Geoscientific Model Development*, **9** (9), 3231–3296, doi:10.5194/gmd-9-3231-2016, URL <https://www.geosci-model-dev.net/9/3231/2016/>.
- Haarsma, R. J., and Coauthors, 2016: High Resolution Model Intercomparison Project (HighResMIP). *Geoscientific Model Development Discussions*, 1–35, doi:10.5194/gmd-2016-66, URL <http://dx.doi.org/10.5194/gmd-2016-66>.
- Hamman, J., B. Nijssen, A. Roberts, A. Craig, W. Maslowski, and R. Osinski, 2017: The coastal streamflow flux in the Regional Arctic System Model. *Journal of Geophysical Research: Oceans*, **122** (3), 1683–1701, doi:10.1002/2016jc012323, URL <http://dx.doi.org/10.1002/2016JC012323>.
- Hammond, M. D., and D. C. Jones, 2016: Freshwater flux from ice sheet melting and iceberg calving in the Southern Ocean. *Geoscience Data Journal*, **3** (2), 60–62, doi:10.1002/gdj3.43, URL <http://dx.doi.org/10.1002/gdj3.43>.
- Hautala, S. L., J. Sprintall, J. T. Potemra, J. C. Chong, W. Pandoe, N. Bray, and A. G. Ilahude, 2001: Velocity structure and transport of the Indonesian Throughflow in the major straits restricting flow into the Indian Ocean. *Journal of Geophysical Research: Oceans*, **106** (C9), 19 527–19 546, doi:10.1029/2000JC000577, URL <https://agupubs.onlinelibrary.wiley.com/doi/abs/10.1029/2000JC000577>, <https://agupubs.onlinelibrary.wiley.com/doi/pdf/10.1029/2000JC000577>.

- Heil, P., R. Massom, I. Allison, and A. Worby, 2011: Physical attributes of sea-ice kinematics during spring 2007 off East Antarctica. *Deep-Sea Research. Part 2: Topical Studies in Oceanography*, **58** (9-10), 1158–1171, doi:10.1016/j.dsr2.2010.12.004, URL <http://ecite.utas.edu.au/76077>, iSSN 0967-0645.
- Hunke, E. C., 2001: Viscous–plastic sea ice dynamics with the EVP model: Linearization issues. *Journal of Computational Physics*, **170** (1), 18–38, doi:10.1006/jcph.2001.6710, URL <http://dx.doi.org/10.1006/jcph.2001.6710>.
- Hunke, E. C., and J. K. Dukowicz, 1997: An elastic–viscous–plastic model for sea ice dynamics. *Journal of Physical Oceanography*, **27** (9), 1849–1867, doi:10.1175/1520-0485(1997)027<1849:aevpmf>2.0.co;2, URL [http://dx.doi.org/10.1175/1520-0485\(1997\)027<1849:AEVPMF>2.0.CO;2](http://dx.doi.org/10.1175/1520-0485(1997)027<1849:AEVPMF>2.0.CO;2).
- Hunke, E. C., and J. K. Dukowicz, 2002: The elastic–viscous–plastic sea ice dynamics model in general orthogonal curvilinear coordinates on a sphere—incorporation of metric terms. *Monthly Weather Review*, **130** (7), 1848–1865, doi:10.1175/1520-0493(2002)130<1848:tevpsi>2.0.co;2, URL [http://dx.doi.org/10.1175/1520-0493\(2002\)130<1848:TEVPSI>2.0.CO;2](http://dx.doi.org/10.1175/1520-0493(2002)130<1848:TEVPSI>2.0.CO;2).
- Hunke, E. C., W. H. Lipscomb, A. K. Turner, N. Jeffery, and S. Elliott, 2015: CICE: the Los Alamos Sea Ice Model documentation and software user’s manual version 5.1. Tech. Rep. LA-CC-06-012, Los Alamos National Laboratory, Los Alamos NM 87545. URL <http://oceans11.lanl.gov/trac/CICE/attachment/wiki/WikiStart/cicedoc.pdf?format=raw>.
- Hutchings, J. K., P. Heil, and W. D. Hibler, 2005: Modeling linear kinematic features in sea ice. *Monthly Weather Review*, **133** (12), 3481–3497, doi:10.1175/mwr3045.1, URL <http://dx.doi.org/10.1175/MWR3045.1>.
- Hutchings, J. K., A. Roberts, C. A. Geiger, and J. Richter-Menge, 2011: Spatial and temporal characterization of sea-ice deformation. *Annals of Glaciology*, **52** (57), 360–368, doi:10.3189/172756411795931769.
- Hutter, N., M. Losch, and D. Menemenlis, 2018: Scaling properties of Arctic sea ice deformation in a high-resolution viscous-plastic sea ice model and in satellite observations. *Journal of Geophysical Research: Oceans*, **123** (1), 672–687, doi:10.1002/2017jc013119, URL <http://dx.doi.org/10.1002/2017JC013119>.
- Ilicak, M., and Coauthors, 2016: An assessment of the Arctic Ocean in a suite of interannual CORE-II simulations. Part III: Hydrography and fluxes. *Ocean Modelling*, **100**, 141–161, doi:10.1016/j.ocemod.2016.02.004, URL <http://dx.doi.org/10.1016/j.ocemod.2016.02.004>.
- Jin, M., and Coauthors, 2018: Effects of model resolution and ocean mixing on forced ice-ocean physical and biogeochemical simulations using global and regional system models. *Journal of Geophysical Research: Oceans*, **123** (1), 358–377, doi:10.1002/2017jc013365, URL <http://dx.doi.org/10.1002/2017JC013365>.
- Kerry, C., B. Powell, M. Roughan, and P. Oke, 2016: Development and evaluation of a high-resolution reanalysis of the East Australian Current region using the Regional Ocean Modelling System (ROMS 3.4) and incremental strong-constraint 4-dimensional variational (IS4D-Var) data assimilation. *Geoscientific Model Development*, **9** (10), 3779–3801, doi:10.5194/gmd-9-3779-2016, URL <http://dx.doi.org/10.5194/gmd-9-3779-2016>.
- Kimmritz, M., S. Danilov, and M. Losch, 2015: On the convergence of the modified elastic–viscous–plastic method for solving the sea ice momentum equation. *Journal of Computational Physics*, **296**, 90–100, doi:10.1016/j.jcp.2015.04.051, URL <http://dx.doi.org/10.1016/j.jcp.2015.04.051>.
- Kimmritz, M., M. Losch, and S. Danilov, 2017: A comparison of viscous-plastic sea ice solvers with and without replacement pressure. *Ocean Modelling*, **115**, 59–69, doi:10.1016/j.ocemod.2017.05.006, URL <http://dx.doi.org/10.1016/j.ocemod.2017.05.006>.

- Kobayashi, S., and Coauthors, 2015: The JRA-55 reanalysis: General specifications and basic characteristics. *Journal of the Meteorological Society of Japan. Ser. II*, **93** (1), 5–48, doi:10.2151/jmsj.2015-001, URL <http://dx.doi.org/10.2151/jmsj.2015-001>.
- Kritsikis, E., M. Aechtner, Y. Meurdesoif, and T. Dubos, 2017: Conservative interpolation between general spherical meshes. *Geoscientific Model Development*, **10** (1), 425–431, doi:10.5194/gmd-10-425-2017, URL <http://dx.doi.org/10.5194/gmd-10-425-2017>.
- Kwok, R., E. C. Hunke, W. Maslowski, D. Menemenlis, and J. Zhang, 2008: Variability of sea ice simulations assessed with RGPS kinematics. *Journal of Geophysical Research*, **113** (C11), doi:10.1029/2008jc004783, URL <http://dx.doi.org/10.1029/2008JC004783>.
- Kwok, R., L. Toudal Pedersen, P. Gudmandsen, and S. S. Pang, 2010: Large sea ice outflow into the Nares Strait in 2007. *Geophysical Research Letters*, **37** (3), doi:10.1029/2009gl041872, URL <http://dx.doi.org/10.1029/2009GL041872>.
- Laurindo, L. C., A. J. Mariano, and R. Lumpkin, 2017: An improved near-surface velocity climatology for the global ocean from drifter observations. *Deep Sea Research Part I: Oceanographic Research Papers*, **124**, 73–92, doi:10.1016/j.dsr.2017.04.009, URL <http://dx.doi.org/10.1016/j.dsr.2017.04.009>.
- Lemieux, J.-F., D. A. Knoll, B. Tremblay, D. M. Holland, and M. Losch, 2012: A comparison of the Jacobian-free Newton–Krylov method and the EVP model for solving the sea ice momentum equation with a viscous-plastic formulation: A serial algorithm study. *Journal of Computational Physics*, **231** (17), 5926–5944, doi:10.1016/j.jcp.2012.05.024, URL <http://dx.doi.org/10.1016/j.jcp.2012.05.024>.
- Lemieux, J.-F., and B. Tremblay, 2009: Numerical convergence of viscous-plastic sea ice models. *Journal of Geophysical Research*, **114** (C5), doi:10.1029/2008jc005017, URL <http://dx.doi.org/10.1029/2008JC005017>.
- Leppäranta, M., 2011: *The Drift of Sea Ice*. 2nd ed., Springer, doi:10.1007/978-3-642-04683-4, URL <https://www.springer.com/gp/book/9783642046827>.
- Lindsay, R. W., J. Zhang, and D. A. Rothrock, 2003: Sea-ice deformation rates from satellite measurements and in a model. *Atmosphere-Ocean*, **41** (1), 35–47, doi:10.3137/ao.410103, URL <http://dx.doi.org/10.3137/ao.410103>.
- Losch, M., and S. Danilov, 2012: On solving the momentum equations of dynamic sea ice models with implicit solvers and the elastic–viscous–plastic technique. *Ocean Modelling*, **41**, 42–52, doi:10.1016/j.ocemod.2011.10.002, URL <http://dx.doi.org/10.1016/j.ocemod.2011.10.002>.
- Losch, M., A. Fuchs, J.-F. Lemieux, and A. Vanselow, 2014: A parallel Jacobian-free Newton–Krylov solver for a coupled sea ice-ocean model. *Journal of Computational Physics*, **257**, 901–911, doi:10.1016/j.jcp.2013.09.026, URL <http://dx.doi.org/10.1016/j.jcp.2013.09.026>.
- Lu, P., Z. Li, B. Cheng, and M. Leppäranta, 2011: A parameterization of the ice-ocean drag coefficient. *Journal of Geophysical Research*, **116** (C7), doi:10.1029/2010jc006878, URL <http://dx.doi.org/10.1029/2010JC006878>.
- Lumpkin, R., and K. Speer, 2007: Global ocean meridional overturning. *Journal of Physical Oceanography*, **37** (10), 2550–2562, doi:10.1175/jpo3130.1, URL <http://dx.doi.org/10.1175/JPO3130.1>.
- Martinson, D. G., and C. Wamser, 1990: Ice drift and momentum exchange in winter Antarctic pack ice. *Journal of Geophysical Research*, **95** (C2), 1741, doi:10.1029/jc095ic02p01741, URL <http://dx.doi.org/10.1029/JC095iC02p01741>.

- Mathiot, P., A. Jenkins, C. Harris, and G. Madec, 2017: Explicit representation and parametrised impacts of under ice shelf seas in the z^* coordinate ocean model NEMO 3.6. *Geoscientific Model Development*, **10** (7), 2849–2874, doi:10.5194/gmd-10-2849-2017, URL <http://dx.doi.org/10.5194/gmd-10-2849-2017>.
- Mazloff, M. R., P. Heimbach, and C. Wunsch, 2010: An eddy-permitting Southern Ocean state estimate. *Journal of Physical Oceanography*, **40** (5), 880–899, doi:10.1175/2009JPO4236.1, URL <http://dx.doi.org/10.1175/2009JPO4236.1>.
- McPhee, M., 2008: *Air-Ice-Ocean Interaction: Turbulent Ocean Boundary Layer Exchange Processes*. Springer New York, doi:10.1007/978-0-387-78335-2, URL <http://dx.doi.org/10.1007/978-0-387-78335-2>.
- Merino, N., N. C. Jourdain, J. Le Sommer, H. Goosse, P. Mathiot, and G. Durand, 2018: Impact of increasing Antarctic glacial freshwater release on regional sea-ice cover in the Southern Ocean. *Ocean Modelling*, **121**, 76–89, doi:10.1016/j.ocemod.2017.11.009, URL <http://dx.doi.org/10.1016/j.ocemod.2017.11.009>.
- Merino, N., J. Le Sommer, G. Durand, N. C. Jourdain, G. Madec, P. Mathiot, and J. Tournadre, 2016: Antarctic icebergs melt over the Southern Ocean: Climatology and impact on sea ice. *Ocean Modelling*, **104**, 99–110, doi:10.1016/j.ocemod.2016.05.001, URL <http://dx.doi.org/10.1016/j.ocemod.2016.05.001>.
- Murray, R. J., 1996: Explicit generation of orthogonal grids for ocean models. *Journal of Computational Physics*, **126** (2), 251–273, doi:10.1006/jcph.1996.0136, URL <http://dx.doi.org/10.1006/jcph.1996.0136>.
- Newsom, E. R., C. M. Bitz, F. O. Bryan, R. Abernathey, and P. R. Gent, 2016: Southern Ocean deep circulation and heat uptake in a high-resolution climate model. *Journal of Climate*, **29** (7), 2597–2619, doi:10.1175/jcli-d-15-0513.1, URL <http://dx.doi.org/10.1175/JCLI-D-15-0513.1>.
- Nihashi, S., and K. I. Ohshima, 2015: Circumpolar mapping of Antarctic coastal polynyas and landfast sea ice: Relationship and variability. *Journal of Climate*, **28** (9), 3650–3670, doi:10.1175/jcli-d-14-00369.1, URL <http://dx.doi.org/10.1175/JCLI-D-14-00369.1>.
- Notz, D., A. Jahn, M. Holland, E. Hunke, F. Massonnet, J. Stroeve, B. Tremblay, and M. Vancoppenolle, 2016: The CMIP6 Sea-Ice Model Intercomparison Project (SIMIP): understanding sea ice through climate-model simulations. *Geoscientific Model Development*, **9** (9), 3427–3446, doi:10.5194/gmd-9-3427-2016, URL <https://www.geosci-model-dev.net/9/3427/2016/>.
- Nye, J. F., 1973: Is there any physical basis for assuming linear viscous behavior for sea ice? *AIDJEX Bull.*, **21**, 18–19, URL http://psc.apl.washington.edu/nonwp_projects/aidjex/files/AIDJEX-21.pdf.
- Ohshima, K. I., S. Nihashi, and K. Iwamoto, 2016: Global view of sea-ice production in polynyas and its linkage to dense/bottom water formation. *Geoscience Letters*, **3** (1), doi:10.1186/s40562-016-0045-4, URL <http://dx.doi.org/10.1186/s40562-016-0045-4>.
- Oke, P. R., and Coauthors, 2013: Evaluation of a near-global eddy-resolving ocean model. *Geoscientific Model Development*, **6** (3), 591–615, doi:10.5194/gmd-6-591-2013, URL <http://www.geosci-model-dev.net/6/591/2013/>.
- Park, H.-S., and A. L. Stewart, 2016: An analytical model for wind-driven Arctic summer sea ice drift. *The Cryosphere*, **10** (1), 227–244, doi:10.5194/tc-10-227-2016, URL <http://dx.doi.org/10.5194/tc-10-227-2016>.

- Rintoul, S. R., 2018: The global influence of localized dynamics in the Southern Ocean. *Nature*, **558 (7709)**, 209–218, doi:10.1038/s41586-018-0182-3, URL <https://doi.org/10.1038/s41586-018-0182-3>.
- Roberts, A., W. Maslowski, J. Jakacki, M. Higgins, A. Craig, J. Cassano, W. Gutowski, and P. Lettenmaier, 2011: High frequency and wavenumber ocean-ice-atmosphere coupling in the Regional Arctic Climate Model. *AGU Fall Meeting Abstracts*, 4.
- Roberts, A., and Coauthors, 2015: Simulating transient ice-ocean Ekman transport in the Regional Arctic System Model and Community Earth System Model. *Annals of Glaciology*, **56 (69)**, 211–228, doi:10.3189/2015aog69a760, URL <http://dx.doi.org/10.3189/2015AoG69A760>.
- Roberts, A. F., and Coauthors, in review 2018: Quality control for community based sea ice model development. *Phil. Trans. Royal Soc. A*.
- Shirasawa, K., and R. G. Ingram, 1997: Currents and turbulent fluxes under the first-year sea ice in resolute passage, northwest territories, canada. *Journal of Marine Systems*, **11 (1-2)**, 21–32, doi:10.1016/s0924-7963(96)00024-3, URL [http://dx.doi.org/10.1016/S0924-7963\(96\)00024-3](http://dx.doi.org/10.1016/S0924-7963(96)00024-3).
- Smeed, D. A., and Coauthors, 2018: The North Atlantic Ocean is in a state of reduced overturning. *Geophysical Research Letters*, **45 (3)**, 1527–1533, doi:10.1002/2017gl076350, URL <http://dx.doi.org/10.1002/2017GL076350>.
- Spence, P., R. M. Holmes, A. M. Hogg, S. M. Griffies, K. D. Stewart, and M. H. England, 2017: Localized rapid warming of West Antarctic subsurface waters by remote winds. *Nature Climate Change*, **7 (8)**, 595–603, doi:10.1038/nclimate3335, URL <http://dx.doi.org/10.1038/nclimate3335>.
- Sprintall, J., S. E. Wijffels, R. Molcard, and I. Jaya, 2009: Direct estimates of the Indonesian Throughflow entering the Indian Ocean: 2004–2006. *Journal of Geophysical Research: Oceans*, **114 (C7)**, doi:10.1029/2008JC005257, URL <http://dx.doi.org/10.1029/2008JC005257>.
- Stewart, K., A. Hogg, S. Griffies, A. Heerdegen, M. Ward, P. Spence, and M. England, 2017: Vertical resolution of baroclinic modes in global ocean models. *Ocean Modelling*, doi:10.1016/j.ocemod.2017.03.012, URL <http://dx.doi.org/10.1016/j.ocemod.2017.03.012>.
- Storkey, D., and Coauthors, 2018: UK Global Ocean GO6 and GO7: a traceable hierarchy of model resolutions. *Geoscientific Model Development Discussions*, 1–43, doi:10.5194/gmd-2017-263, URL <http://dx.doi.org/10.5194/gmd-2017-263>.
- Suzuki, T., D. Yamazaki, H. Tsujino, Y. Komuro, H. Nakano, and S. Urakawa, 2017: A dataset of continental river discharge based on JRA-55 for use in a global ocean circulation model. *Journal of Oceanography*, doi:10.1007/s10872-017-0458-5, URL <https://doi.org/10.1007/s10872-017-0458-5>.
- Talley, L. D., 2013: Closure of the global overturning circulation through the Indian, Pacific, and Southern Oceans: Schematics and transports. *Oceanography*, **26 (1)**, 80–97, doi:10.5670/oceanog.2013.07, URL <https://doi.org/10.5670/oceanog.2013.07>.
- Tamura, T., and K. I. Ohshima, 2011: Mapping of sea ice production in the Arctic coastal polynyas. *Journal of Geophysical Research*, **116 (C7)**, doi:10.1029/2010jc006586, URL <http://dx.doi.org/10.1029/2010JC006586>.
- Tamura, T., K. I. Ohshima, A. D. Fraser, and G. D. Williams, 2016: Sea ice production variability in Antarctic coastal polynyas. *Journal of Geophysical Research: Oceans*, **121 (5)**, 2967–2979, doi:10.1002/2015jc011537, URL <http://dx.doi.org/10.1002/2015JC011537>.
- Tamura, T., K. I. Ohshima, and S. Nishihashi, 2008: Mapping of sea ice production for Antarctic coastal polynyas. *Geophysical Research Letters*, **35 (7)**, n/a–n/a, doi:10.1029/2007gl032903, URL <http://dx.doi.org/10.1029/2007GL032903>.

- Toyota, T., and N. Kimura, 2018: An examination of the sea ice rheology for seasonal ice zones based on ice drift and thickness observations. *Journal of Geophysical Research: Oceans*, doi:10.1002/2017JC013627, URL <http://dx.doi.org/10.1002/2017JC013627>.
- Tsamados, M., D. L. Feltham, and A. V. Wilchinsky, 2013: Impact of a new anisotropic rheology on simulations of Arctic sea ice. *Journal of Geophysical Research: Oceans*, **118** (1), 91–107, doi:10.1029/2012jc007990, URL <http://dx.doi.org/10.1029/2012JC007990>.
- Tseng, Y.-h., and Coauthors, 2016: North and equatorial Pacific Ocean circulation in the CORE-II hindcast simulations. *Ocean Modelling*, **104**, 143–170, doi:10.1016/j.ocemod.2016.06.003, URL <http://dx.doi.org/10.1016/j.ocemod.2016.06.003>.
- Tsujino, H., 2015a: On the use of JRA55 for driving ocean-sea ice models - biases, correction (adjustment), results from preliminary model run. *OMDP forcing mini workshop 29-30 Jan 2015, Grenoble, France*, URL http://www.clivar.org/sites/default/files/documents/wgomd/grenoble2015/OMDP_Grenoble2015.Tsujino.pdf.
- Tsujino, H., 2015b: Short description of a JRA-55 based surface atmospheric data set for driving ocean-sea ice models. Tech. rep., JMA Meteorological Research Institute. URL <https://mri-2.mri-jma.go.jp/owncloud/index.php/s/3d33d5a6ee3bd326abae2cecbea91bd0#pdfviewer>.
- Tsujino, H., 2016: JRA-55 based surface atmospheric data set for driving ocean-sea ice models. *OMDP extended meeting 14 January 2016, JAMSTEC, Yokohama, Japan*, URL http://www.clivar.org/sites/default/files/documents/wgomd/japan2016/OMDP_Meeting/Tsujino_OMDP2016.pdf.
- Tsujino, H., and Coauthors, 2016: JRA-55 based data set for driving ocean - sea ice model (JRA55-do). 17 September 2016 ARP-OMDP joint session Qingdao, China.
- Tsujino, H., and Coauthors, 2018a: JRA-55 based surface dataset for driving ocean-sea-ice models (JRA55-do). *Ocean Modelling* (submitted).
- Tsujino, H., and Coauthors, 2018b: *User manual for JRA-55 based surface dataset for driving ocean-sea-ice models (JRA55-do)*. URL <https://mri-2.mri-jma.go.jp/owncloud/index.php/s/cSntssoesw4ATRT>.
- Turner, A. K., E. C. Hunke, and C. M. Bitz, 2013: Two modes of sea-ice gravity drainage: A parameterization for large-scale modeling. *Journal of Geophysical Research: Oceans*, **118** (5), 2279–2294, doi:10.1002/jgrc.20171, URL <http://dx.doi.org/10.1002/jgrc.20171>.
- Uotila, P., S. O'Farrell, S. J. Marsland, and D. Bi, 2013: The sea-ice performance of the Australian climate models participating in the CMIP5. *Australian Meteorological And Oceanographic Journal*, **63** (1), 121–143.
- Urrego-Blanco, J. R., N. M. Urban, E. C. Hunke, A. K. Turner, and N. Jeffery, 2016: Uncertainty quantification and global sensitivity analysis of the Los Alamos sea ice model. *Journal of Geophysical Research: Oceans*, **121** (4), 2709–2732, doi:10.1002/2015jc011558, URL <http://dx.doi.org/10.1002/2015JC011558>.
- Wang, K., and C. Wang, 2009: Modeling linear kinematic features in pack ice. *Journal of Geophysical Research*, **114** (C12), doi:10.1029/2008jc005217, URL <http://dx.doi.org/10.1029/2008JC005217>.
- Wang, Q., S. Danilov, T. Jung, L. Kaleschke, and A. Wernecke, 2016a: Sea ice leads in the arctic ocean: Model assessment, interannual variability and trends. *Geophysical Research Letters*, **43** (13), 7019–7027, doi:10.1002/2016gl068696, URL <http://dx.doi.org/10.1002/2016GL068696>.
- Wang, Q., and Coauthors, 2016b: An assessment of the Arctic Ocean in a suite of interannual CORE-II simulations. Part I: Sea ice and solid freshwater. *Ocean Modelling*, **99**, 110–132, doi:10.1016/j.ocemod.2015.12.008, URL <http://dx.doi.org/10.1016/j.ocemod.2015.12.008>.

- Wang, Q., and Coauthors, 2016c: An assessment of the Arctic Ocean in a suite of interannual CORE-II simulations. Part II: Liquid freshwater. *Ocean Modelling*, **99**, 86–109, doi:10.1016/j.ocemod.2015.12.009, URL <http://dx.doi.org/10.1016/j.ocemod.2015.12.009>.
- Waters, J. K., and M. S. Bruno, 1995: Internal wave generation by ice floes moving in stratified water: Results from a laboratory study. *Journal of Geophysical Research*, **100** (C7), 13 635, doi:10.1029/95jc01220, URL <http://dx.doi.org/10.1029/95JC01220>.
- Weiss, J., and E. M. Schulson, 2009: Coulombic faulting from the grain scale to the geophysical scale: lessons from ice. *Journal of Physics D: Applied Physics*, **42** (21), 214 017, URL <http://stacks.iop.org/0022-3727/42/i=21/a=214017>.
- Weiss, J., E. M. Schulson, and H. L. Stern, 2007: Sea ice rheology from in-situ, satellite and laboratory observations: Fracture and friction. *Earth and Planetary Science Letters*, **255** (1-2), 1–8, doi:10.1016/j.epsl.2006.11.033, URL <http://dx.doi.org/10.1016/j.epsl.2006.11.033>.
- Wijeratne, S., C. Pattiaratchi, and R. Proctor, 2018: Estimates of surface and subsurface boundary current transport around Australia. *Journal of Geophysical Research: Oceans*, doi:10.1029/2017jc013221, URL <http://dx.doi.org/10.1029/2017JC013221>.
- Wilchinsky, A. V., and D. L. Feltham, 2006: Modelling the rheology of sea ice as a collection of diamond-shaped floes. *Journal of Non-Newtonian Fluid Mechanics*, **138** (1), 22–32, doi:10.1016/j.jnnfm.2006.05.001, URL <http://dx.doi.org/10.1016/j.jnnfm.2006.05.001>.
- Wu, Y., X. Zhai, and Z. Wang, 2017: Decadal-mean impact of including ocean surface currents in bulk formulas on surface air-sea fluxes and ocean general circulation. *Journal of Climate*, **30** (23), 9511–9525, doi:10.1175/jcli-d-17-0001.1, URL <http://dx.doi.org/10.1175/JCLI-D-17-0001.1>.
- Xu, Y., and L.-L. Fu, 2011: Global variability of the wavenumber spectrum of oceanic mesoscale turbulence. *Journal of Physical Oceanography*, **41** (4), 802–809, doi:10.1175/2010JPO4558.1, URL <http://dx.doi.org/10.1175/2010JPO4558.1>.